

Estimation of oblique electroweak corrections

Michael E. Peskin and Tatsu Takeuchi

Stanford Linear Accelerator Center, Stanford University, Stanford, California 94309

(Received 9 December 1991)

We review the general analysis of the contributions of electroweak vacuum-polarization diagrams to precision experiments. We first review the representation of these contributions by three parameters S , T , and U and discuss the assumptions involved in this reduction. We then discuss the contributions to these parameters from various models of new physics. We show that S can be computed by a dispersion relation, and we use this technique to estimate S in technicolor models of the Higgs sector. We discuss the reliability and the gauge invariance of this estimate. Finally, we present the limits on S and T imposed by current experimental results.

PACS number(s): 12.15.Cc, 12.15.Ji, 12.50.Lr

I. INTRODUCTION

While no one seriously doubts the validity of the $SU(2)_L \times U(1)_Y$ gauge theory of electroweak interactions, the nature of the Higgs sector which is responsible for breaking the $SU(2)_L \times U(1)_Y$ symmetry, and thus giving the W 's and the Z^0 their masses, is still a mystery. A variety of theories, from the minimal model with one scalar doublet to technicolor models with elaborate dynamics, have been proposed, but none of the new particle states predicted by these theories has yet been observed.

Since experiment has not yet offered direct evidence to distinguish these theories, it is important to make the best use of all sources of indirect information that current measurements provide. The most important of these indirect constraints come from precision measurements of weak-interaction parameters. In the past year, these measurements have reached the level of 1% accuracy in the determination of the W mass and the parameters of the Z^0 resonance. Measurements at this level already allow us to distinguish among different models of the Higgs sector.

The most general models of the Higgs sector allow for large deviations from the predictions of the minimal version of the standard model. However, more than ten years ago, Veltman [1,2] pointed out the relevance of the natural zeroth-order relation of the minimal standard model:

$$\rho \equiv \frac{m_W^2}{m_Z^2 \cos^2 \theta_W} = 1. \quad (1.1)$$

Experimentally, this relation is satisfied to better than 1%, so that it is reasonable to assume that the corrections to this relation arise only from radiative corrections. That requirement restricts the nature of the Higgs sector [forbidding, for example, expectation values for scalars which transform as $SU(2)$ triplets]. However, Sikivie, Susskind, Voloshin, and Zakharov [3] have argued that (1.1) is naturally valid up to electroweak radiative corrections in a large class of models in which the Higgs sector has an unbroken $SU(2)$ global symmetry,

called by these authors a *custodial* symmetry. Large deviations from the predictions of the minimal standard model can also occur if the gauge structure of the model is extended, so that there exists a new neutral boson Z^0 which mixes with the Z^0 . In this paper we will restrict our attention to models with only $SU(2) \times U(1)$ gauge bosons and in which (1.1) is a natural relation. This case still includes the full variety of models of the Higgs sector. We will show how to distinguish these models by comparing the values predicted for their radiative corrections with those obtained from experiment.

In models in which the Higgs sector is weakly interacting, the computation of the electroweak radiative corrections due to the Higgs particles is a straightforward endeavor involving only ordinary perturbation theory. However, we would also like to discuss models, such as technicolor, in which the Higgs sector is strongly interacting. In this case, we face not only the practical problem that perturbation theory is unreliable but also the conceptual problem that the massless Goldstone bosons which play an essential role in the Higgs mechanism do not appear in any purely perturbative approach.

In this paper, we will argue that this problem is naturally solved by the use of dispersion relations. We will relate the experimentally relevant electroweak corrections to dispersive integrals over the states of the Higgs sector and illustrate the theoretical evaluation of these integrals in some cases of interest. We will also explain how the values of these integrals for the true Higgs sector can be extracted from experimental data. We expect that, as the values of these dispersive integrals are determined experimentally, they will become important integral constraints on the content of the Higgs sector. Already, experiment can exclude technicolor models with large strongly interacting sectors, independently of any considerations of extended technicolor, quark mass generation, or flavor-changing neutral currents. We will argue carefully to this conclusion in the course of this paper.

Some of the analysis of this paper is new, but a large part of our intent is to collect a number of results from the literature and to explain them clearly in a unified way. The idea that the Higgs sector is constrained by

precision electroweak experiments was, of course, originated by Veltman [1,2]. Many authors have studied the detailed effects of the Higgs boson of the minimal standard model in electroweak corrections; the current status of this subject and a review of the literature may be found in the valuable 1989 study volume [4] for the CERN e^+e^- collider LEP. The effects of technicolor models of the Higgs sector have been computed by the two of us in collaboration with Renken [5], Lynn and Stuart [6], and Appelquist, Einhorn, and Wijewardhana [7], and more recently by Golden and Randall [8], Holdom and Terning [9], Johnson, Young, and McKay [10], and Dobado, Espriu, and Herrero [11]. Though most papers on technicolor model building stress the constraint of the ρ parameter, even Ref. [5] made clear that the pattern of weak-interaction renormalizations due to technicolor is more complicated, and cannot be summarized in a single parameter.

In parallel with these model-dependent studies, the authors of Ref. [6] suggested that one could probe for the effects of new physics in electroweak corrections in a general way, by concentrating on the effects of vacuum-polarization diagrams (*oblique* corrections) and searching for these effects independently of the underlying model. This idea was incorporated into a complete theory of weak radiative corrections by Kennedy and Lynn [12]. This Kennedy-Lynn formalism has had an important influence in providing a language which is simultaneously precise and conceptually transparent for describing the results of experiments on electroweak corrections.

Most recently, we proposed a simple two-parameter representation of the effects of oblique electroweak corrections, in a form appropriate for a direct comparison with experiment [13]. This representation was obtained by approximating the Kennedy-Lynn formalism in a manner appropriate for corrections due to particles of very large mass. We argued that one of these parameters could be represented by a dispersive integral and thus could be readily estimated in models with a strongly interacting Higgs sector. Our parametrization has subsequently been discussed, extended, and analyzed by several groups [14–18]. Since all of the papers of Refs. [13–18] are brief communications, we feel that there is a need for a comprehensive review of these recent developments.

In this paper, then, we will review the parametrization of oblique electroweak corrections and the evaluation of these corrections by dispersion relations. In Sec. II, we will review the Kennedy-Lynn parametrization of electroweak corrections. In Sec. III, we will analyze a subset of the Kennedy-Lynn parameters which give the corrections to the most important weak-interaction observables. We will present general formulas for the renormalization of these parameters in terms of vacuum-polarization amplitudes. Then we will show how these formulas can be reduced to linear functions of two parameters S and T . In Sec. IV, we will study the example of electroweak radiative corrections due to a heavy fermion doublet to illustrate the approximations involved in this reduction. This example will also clarify the physical significance of these parameters: T quantifies the strength of weak-isospin breaking through the radiative corrections (including the

familiar effect of the top quark proportional to m_t^2/m_Z^2), while S is an isospin-symmetric measure of the size of the Higgs sector.

Sections V–VII will discuss the estimation of oblique corrections for the case of a strongly interacting Higgs sector. In Sec. V, we will present a formula for S in terms of a dispersive integral. In Sec. VI, we will discuss the gauge invariance of this expression, emphasizing the subtleties which arise when the Goldstone bosons appear only nonperturbatively. In Sec. VII, we will evaluate the dispersive integral for S in simple technicolor models and discuss the accuracy of this estimate for more realistic models including extended technicolor. In Sec. VIII, we will briefly remark on the estimation of the parameter T . We have not been able to obtain a reliable dispersive formula for T ; this remains an important open problem.

In Sec. IX, we will discuss the current experimental constraints on S and T . We will first review the sensitivity of various precision weak-interactions measurements to S and T . We will show that the various measurements fall into three general classes: those sensitive mainly to T , those equally sensitive to T and S , and those mainly sensitive to S . The first class includes all of the best-known weak-interaction observables: m_W , the ratio of neutral-to charged-current neutrino cross sections R_ν , and the width of the Z^0 . The second class includes the weak-interaction asymmetries at the Z^0 peak: A_{LR} and A_{FB} . The third class, which gives a direct restriction on S , includes the magnitude of parity violation in atomic physics [14]. We will show that combining these three classes of experiments already places quite a strong constraint on S and T . We will discuss the improvement in this constraint which can be expected from future experiments. At a marginal level of significance, the current data favor a sizable negative value of S . This result is surprising, and, if confirmed, would be very problematic to reconcile with simple extensions of the standard model. On the other hand, this result already excludes technicolor models, which produce positive contributions to S , if the technicolor sectors of these models are sufficiently large. In Sec. X, we will present some general conclusions.

II. FORMALISM OF OBLIQUE CORRECTIONS

In this section, we review the general formalism developed by Kennedy and Lynn [12] for treating radiative corrections to weak-interaction processes with light external fermions. While the formalism of Kennedy and Lynn encompasses radiative corrections from physics both within and beyond the standard model, we will only be considering the latter. Therefore, we will not go into the subtleties that must be taken into account for the standard-model corrections. In this paper, we will not be trying to improve upon or even reproduce the full results of Kennedy and Lynn, which are already highly accurate perturbative computations. Rather, we wish to simplify their formalism by seeking approximations which do not compromise this accuracy excessively while making the results as transparent as possible.

We concentrate on weak-interaction processes involving only light fermions as external particles since those

are the only processes accessible to present day experiments. As pointed out by the authors of Refs. [6,12], this restriction has some important consequences which simplifies our analysis considerably. The first is that we can neglect the terms proportional to $q^\mu q^\nu$ in the W and Z propagators. This is because contraction with the external fermion currents suppresses the $q^\mu q^\nu$ terms compared to the $g^{\mu\nu}$ terms by a factor of (m_f^2/m_Z^2) where m_f is the external fermion mass. (The $q^\mu q^\nu$ term of the photon propagator has no effect, due to the Ward identity.) The second is that we can assume that radiative corrections due to physics beyond the standard model appear dominantly through vacuum polarizations (oblique corrections) and that vertex corrections and box diagrams (direct corrections) can be neglected [19]. For example, modifications of the Higgs sector give vacuum-polarization corrections of order α while vertex corrections and box diagrams are suppressed again by an additional factor of (m_f^2/m_Z^2) . The rule of thumb here is that we can neglect anything that goes to zero in the limit $m_f \rightarrow 0$. For another example, the effects of new heavy quarks and leptons on the properties of the Z and W bosons enter only through vacuum-polarization diagrams. When we discuss the dynamical Higgs sector of technicolor models, we will need to argue that it is consistent with gauge invariance to neglect the vertex and box diagrams containing the Goldstone bosons absorbed by the W and Z in the Higgs mechanism. We will defer this point to Sec. VI. In this section, we will assume that the effects of the new physics are purely oblique and work out the consequences of that assumption.

We start by introducing some notation. J_Q^μ, J_3^μ , and $J_\pm^\mu = J_1^\mu \pm iJ_2^\mu$ denote the electromagnetic and weak-isospin currents coupling to the electroweak gauge bosons via

$$\frac{e}{\sqrt{2}s}(W_\mu^+ J_+^\mu + W_\mu^- J_-^\mu) + \frac{e}{sc} Z_\mu (J_3^\mu - s^2 J_Q^\mu) + e A_\mu J_Q^\mu, \quad (2.1)$$

where $s = \sin\theta_W$ and $c = \cos\theta_W$.

We denote the coefficient of $g^{\mu\nu}$ in the photon, Z , and W propagators by G_{AA} , G_{ZZ} , and G_{WW} , respectively, and that of the photon- Z mixing by G_{ZA} . Then, the matrix elements of the charged- and neutral-current interactions mediated by the electroweak gauge bosons can be written formally as

$$\begin{aligned} \mathcal{M}_{\text{NC}} &= e^2 Q Q' G_{AA} \\ &+ \frac{e^2}{sc} [Q(I_3' - s^2 Q') + (I_3 - s^2 Q) Q'] G_{ZA} \\ &+ \frac{e^2}{s^2 c^2} (I_3 - s^2 Q)(I_3' - s^2 Q') G_{ZZ}, \\ \mathcal{M}_{\text{CC}} &= \frac{e^2}{2s^2} I_+ I_- G_{WW}, \end{aligned} \quad (2.2)$$

where (I_3, Q) and (I_3', Q') are the SU(2) and electric charges of the external fermions and I_\pm are the isospin-raising and -lowering matrices.

To leading order, the propagator G_{ZA} vanishes and the

other three propagators are given by

$$D_{BB} = \frac{1}{q^2 - m_{0B}^2}, \quad (2.3)$$

for $B = A, Z, W$, with the bare masses

$$m_{0A}^2 = 0, \quad m_{0Z}^2 = \frac{e^2 v^2}{s^2 c^2} \frac{v^2}{4}, \quad m_{0W}^2 = \frac{e^2 v^2}{s^2} \frac{v^2}{4}. \quad (2.4)$$

These expressions are constructed to satisfy the natural relation (1.1).

Vacuum polarizations affect the above interactions by modifying the gauge-boson propagators G_{AA} , G_{ZA} , G_{ZZ} , and G_{WW} . This is the reason why they are called ‘‘oblique’’ corrections as opposed to the ‘‘direct’’ vertex and box corrections which modify the form of the interactions themselves. We define the vacuum-polarization amplitudes $\Pi_{XY}(q^2)$, where $(XY) = (11), (22), (33), (3Q)$, and (QQ) , by

$$ig^{\mu\nu} \Pi_{XY}(q^2) + (q^\mu q^\nu \text{ terms}) \equiv \int d^4x e^{-iqx} \langle J_X^\mu(x) J_Y^\nu(0) \rangle. \quad (2.5)$$

It is useful to define $\Pi'_{XY}(q^2)$ by

$$\Pi_{XY}(q^2) \equiv \Pi_{XY}(0) + q^2 \Pi'_{XY}(q^2). \quad (2.6)$$

Note that $\Pi'_{XY}(q^2)$ is equal to $d\Pi_{XY}/dq^2$ only at $q^2=0$. The unbroken U(1) symmetry of electromagnetism implies that $\Pi_{11}(q^2) = \Pi_{22}(q^2)$. The QED Ward identity implies further that $\Pi_{3Q}(0) = \Pi_{QQ}(0) = 0$. Therefore, $\Pi_{QQ}(q^2) = q^2 \Pi'_{QQ}(q^2)$ and $\Pi_{3Q}(q^2) = q^2 \Pi'_{3Q}(q^2)$.

We further define the following shorthand notations for the combinations of Π 's that make up the one-particle irreducible (1PI) self-energies of the photon, W , and Z , and the 1PI photon- Z mixing, shown in Fig. 1:

$$\begin{aligned} \Pi_{AA} &= e^2 \Pi_{QQ}, \quad \Pi_{ZA} = \frac{e^2}{sc} (\Pi_{3Q} - s^2 \Pi_{QQ}), \\ \Pi_{ZZ} &= \frac{e^2}{s^2 c^2} (\Pi_{33} - 2s^2 \Pi_{3Q} + s^4 \Pi_{QQ}), \\ \Pi_{WW} &= \frac{e^2}{s^2} \Pi_{11}. \end{aligned} \quad (2.7)$$

Kennedy and Lynn were careful to include the effects of the vacuum-polarization amplitudes to all orders, using the Dyson equations for the propagators G_{AB} : namely

$$\begin{aligned} G_{AA} &= D_{AA} + D_{AA} \Pi_{AA} G_{AA}, \\ G_{ZA} &= D_{ZZ} \Pi_{ZA} G_{AA}, \\ G_{ZZ} &= D_{ZZ} + D_{ZZ} \Pi_{ZZ} G_{ZZ}, \\ G_{WW} &= D_{WW} + D_{WW} \Pi_{WW} G_{WW}, \end{aligned} \quad (2.8)$$

where D_{AA} , D_{ZZ} , and D_{WW} are the bare propagators (2.3). If we insert the solution to these Dyson equations into (2.2), we find an expression equal to

$$\mathcal{M}_{\text{NC}} = e^2 \frac{QQ'}{q^2 - \Pi_{AA}} + \frac{e^2}{s^2 c^2} \frac{\left[I_3 - \left[s^2 - sc \frac{\Pi_{ZA}}{q^2 - \Pi_{AA}} \right] Q \right] \left[I'_3 - \left[s^2 - sc \frac{\Pi_{ZA}}{q^2 - \Pi_{AA}} \right] Q' \right]}{q^2 - m_{0Z}^2 - \Pi_{ZZ} - \frac{(\Pi_{ZA})^2}{q^2 - \Pi_{AA}}}, \quad (2.9)$$

$$\mathcal{M}_{\text{CC}} = \frac{e^2}{2s^2} \frac{I_+ + I_-}{q^2 - m_{0W}^2 - \Pi_{WW}}.$$

Following Kennedy and Lynn, we define the running couplings $e_*^2(q^2)$ and $s_*^2(q^2)$ as

$$e_*^2(q^2) \equiv \frac{e^2}{1 - e^2 \Pi'_{QQ}(q^2)} = e^2 [1 + e^2 \Pi'_{QQ}(q^2)], \quad (2.10)$$

$$s_*^2(q^2) \equiv s^2 - sc \frac{\Pi_{ZA}(q^2)}{q^2 - \Pi_{AA}(q^2)} = s^2 - e^2 [\Pi'_{3Q}(q^2) - s^2 \Pi'_{QQ}(q^2)].$$

It suffices to keep only the terms linear in the Π 's, since we are concerned with nonstandard corrections which are very small. Equation (2.9) can then be recast into

$$\mathcal{M}_{\text{NC}} = e_*^2 Q \frac{1}{q^2} Q' + \frac{e^2}{s^2 c^2} (I_3 - s_*^2 Q) \frac{1}{q^2 - \frac{e^2}{s^2 c^2} \left[\frac{v^2}{4} + (\Pi_{33} - 2s^2 \Pi_{3Q} + s^4 \Pi_{QQ}) \right]} (I'_3 - s_*^2 Q'), \quad (2.11)$$

$$\mathcal{M}_{\text{CC}} = \frac{e^2}{2s^2} I_+ + \frac{1}{q^2 - \frac{e^2}{s^2} \left[\frac{v^2}{4} + \Pi_{11} \right]} I_-.$$

We have omitted terms that are quadratic and higher order in the Π 's from the denominator of the Z propagator.

The W and Z masses are the poles of their respective propagators. Therefore, from (2.11) we see that

$$m_Z^2 = \frac{e^2}{s^2 c^2} \frac{v^2}{4} + \frac{e^2}{s^2 c^2} (\Pi_{33} - 2s^2 \Pi_{3Q} + s^4 \Pi_{QQ})(m_Z^2), \quad (2.12)$$

$$m_W^2 = \frac{e^2}{s^2} \frac{v^2}{4} + \frac{e^2}{s^2} \Pi_{11}(m_W^2).$$

Define the wave-function renormalization constants Z_Z and Z_W as the coefficients of the poles in the Z and W propagators:

$$Z_Z^{-1} = 1 - \frac{e^2}{s^2 c^2} \frac{d}{dq^2} (\Pi_{33} - 2s^2 \Pi_{3Q} + s^4 \Pi_{QQ}) \Big|_{q^2=m_Z^2}, \quad (2.13)$$

$$Z_W^{-1} = 1 - \frac{e^2}{s^2} \frac{d}{dq^2} \Pi_{11} \Big|_{q^2=m_W^2},$$

It is useful to define running masses $M_{Z*}^2(q^2)$ and $M_{W*}^2(q^2)$ by

$$\frac{1}{q^2 - \frac{e^2}{s^2 c^2} \left[\frac{v^2}{4} + (\Pi_{33} - 2s^2 \Pi_{3Q} + s^4 \Pi_{QQ}) \right]} = \frac{Z_Z}{q^2 - M_{Z*}^2},$$

$$\frac{1}{q^2 - \frac{e^2}{s^2} \left[\frac{v^2}{4} + \Pi_{11} \right]} = \frac{Z_W}{q^2 - M_{W*}^2}; \quad (2.14)$$

FIG. 1. Definition of the basic electroweak vacuum-polarization amplitudes.

these running masses satisfy

$$M_{Z^*}^2(m_Z^2) = m_Z^2, \quad \frac{d}{dq^2} M_{Z^*}^2 \Big|_{q^2=m_Z^2} = 0, \quad M_{W^*}^2(m_W^2) = m_W^2, \quad \frac{d}{dq^2} M_{W^*}^2 \Big|_{q^2=m_W^2} = 0. \quad (2.15)$$

With these definitions, we can rewrite (2.11) in a compact form as

$$\mathcal{M}_{\text{NC}} = e_*^2 Q \frac{1}{q^2} Q' + \frac{e^2}{s_*^2 c_*^2} (I_3 - s_*^2 Q) \frac{Z_Z}{q^2 - M_{Z^*}^2} (I_3' - s_*^2 Q'), \quad \mathcal{M}_{\text{CC}} = \frac{e^2}{2s_*^2} I_+ + \frac{Z_W}{q^2 - M_{W^*}^2} I_-. \quad (2.16)$$

We take one more step and define the running wave-function renormalization constants $Z_{Z^*}(q^2)$ and $Z_{W^*}(q^2)$ by [20]

$$\frac{e_*^2}{s_*^2 c_*^2} Z_{Z^*} \equiv \frac{e^2}{s^2 c^2} Z_Z, \quad \frac{e_*^2}{s_*^2} Z_{W^*} \equiv \frac{e^2}{s^2} Z_W, \quad (2.17)$$

where $c_*^2 \equiv 1 - s_*^2$. In terms of the Π 's, they are expressed as

$$\begin{aligned} Z_{Z^*} &= Z_Z \left[1 - e^2 \Pi'_{QQ}(q^2) - \frac{e^2(c^2 - s^2)}{s^2 c^2} [\Pi'_{3Q}(q^2) - s^2 \Pi'_{QQ}(q^2)] \right] \\ &= 1 + \frac{e^2}{s^2 c^2} \frac{d}{dq^2} (\Pi_{33} - 2s^2 \Pi_{3Q} + s^4 \Pi_{QQ}) \Big|_{q^2=m_Z^2} - \frac{e^2 s^2}{c^2} \Pi'_{QQ}(q^2) - \frac{e^2(c^2 - s^2)}{s^2 c^2} \Pi'_{3Q}(q^2), \\ Z_{W^*} &= Z_W \left[1 - e^2 \Pi'_{QQ}(q^2) - \frac{e^2}{s^2} [\Pi'_{3Q}(q^2) - s^2 \Pi'_{QQ}(q^2)] \right] \\ &= 1 + \frac{e^2}{s^2} \frac{d}{dq^2} \Pi_{11} \Big|_{q^2=m_W^2} - \frac{e^2}{s^2} \Pi'_{3Q}(q^2). \end{aligned} \quad (2.18)$$

The final result of these rearrangements is

$$\begin{aligned} \mathcal{M}_{\text{NC}} &= e_*^2 Q \frac{1}{q^2} Q' \\ &\quad + \frac{e_*^2}{s_*^2 c_*^2} (I_3 - s_*^2 Q) \frac{Z_{Z^*}}{q^2 - M_{Z^*}^2} (I_3' - s_*^2 Q'), \\ \mathcal{M}_{\text{CC}} &= \frac{e_*^2}{2s_*^2} I_+ + \frac{Z_{W^*}}{q^2 - M_{W^*}^2} I_-, \end{aligned} \quad (2.19)$$

where all starred quantities are now functions of q^2 . In Ref. [12], Kennedy and Lynn showed that, with a proper definition of the starred functions, this definition is correct to all orders in vacuum polarizations and also subsumes the major part of the standard-model direct corrections.

The final equations (2.19) have exactly the same form as the tree-level amplitudes, except that all the coupling constants and gauge-boson parameters are replaced by starred parameters. What this shows is that the *oblique* corrections affect weak-interaction observables only via the starred functions. In other words, given an observable in terms of bare parameters at the tree level, we only need to replace the bare parameters with their starred counterparts evaluated at the appropriate momentum to incorporate the corrections from vacuum-polarization diagrams. For instance, the obliquely corrected left-right asymmetry A_{LR} will be given by

$$A_{LR}(q^2) = \frac{2[1 - 4s_*^2(q^2)]}{1 + [1 - 4s_*^2(q^2)]^2}. \quad (2.20)$$

The Z width will be given by

$$\Gamma_Z = Z_{Z^*} \frac{\alpha_* m_Z}{6s_*^2 c_*^2} \sum_f (I_{3f} - s_*^2 Q_f) N_f \Big|_{q^2=m_Z^2}, \quad (2.21)$$

where $\alpha_*(q^2) \equiv e_*^2(q^2)/4\pi$, and N_f is the effective number of colors of the fermion flavor f : For leptons $N_f = 1$; for quarks

$$\begin{aligned} N_f &= N_{\text{quark}} \equiv 3 \left[1 + \frac{\alpha_s}{\pi} + \dots \right] \\ &= 3.12 \pm 0.01 \quad \text{at } q^2 = m_Z^2, \end{aligned} \quad (2.22)$$

corresponding to $\alpha_s(m_Z^2) = 0.12 \pm 0.01$. We can assess the effects of oblique corrections on these observables through the effects of these corrections on the starred functions, which are simply described by the relations (2.10), (2.18). Of course, A_{LR} and Γ_Z also receive corrections from physics within the standard model which are nonoblique. Kennedy and Lynn have shown that the most important part of these corrections can also be stuffed into the starred functions. The initial-state radiative corrections to the Z^0 parameters are large and must be separately assessed. However, the remaining nonoblique corrections are small, only a few tenths of a percent, at the Z pole and below. Therefore, the starred functions are extremely useful tools to summarize the effects of radiative corrections both from within and beyond the standard model.

While (2.19) contains all the information necessary to see how various observables are corrected over the range of energies, it is somewhat cumbersome to apply to low-energy experiments. Therefore, let us return to (2.11) and take the limit $q^2 \rightarrow 0$. The Z and W exchange parts of (2.11) in this limit are

$$\begin{aligned} \mathcal{M}_{\text{NC}} &= -[I_3 - s_*^2(0)Q] \frac{1}{\left[\frac{v^2}{4} + \Pi_{33}(0)\right]} [I'_3 - s_*^2(0)Q'] , \\ \mathcal{M}_{\text{CC}} &= -\frac{1}{2}I_+ \frac{1}{\left[\frac{v^2}{4} + \Pi_{11}(0)\right]} I_- . \end{aligned} \quad (2.23)$$

These matrix elements should be compared with the standard form of the low-energy effective Lagrangian of weak interactions:

$$\mathcal{L}_{\text{eff}} = -\frac{4G_F}{\sqrt{2}} \{J_+^\mu J_-^\mu + \rho_*(0)[J_3^\mu - s_*^2(0)J_Q^\mu]^2\} , \quad (2.24)$$

We denote the low-energy ratio of charged- to neutral-current amplitudes by $\rho_*(0)$, to avoid confusion with the Veltman definition (1.1). We can now make the identifications

$$\begin{aligned} \frac{1}{4\sqrt{2}G_F} &= \frac{v^2}{4} + \Pi_{11}(0) , \\ \frac{1}{\rho_*(0)} &= \frac{\frac{v^2}{4} + \Pi_{33}(0)}{\frac{v^2}{4} + \Pi_{11}(0)} \\ &= 1 - 4\sqrt{2}G_F[\Pi_{11}(0) - \Pi_{33}(0)] . \end{aligned} \quad (2.25)$$

The predictions of weak-interaction theory for low-energy experiments are expressed through the parameters of the low-energy effective Lagrangian, and so relations (2.25) and (2.10) for $s_*^2(0)$ codify the dependence of these predictions on oblique corrections. For example, the factors g_L^2 and g_R^2 that relate the ratios of cross sections in deep-inelastic neutrino scattering experiments,

$$R_\nu = g_L^2 + r g_R^2, \quad R_{\bar{\nu}} = g_L^2 + \frac{g_R^2}{r} , \quad (2.26)$$

where

$$\begin{aligned} R_\nu &= \frac{\sigma(\nu_\mu N \rightarrow \nu_\mu X)}{\sigma(\nu_\mu N \rightarrow \mu^- X)} , \\ R_{\bar{\nu}} &= \frac{\sigma(\bar{\nu}_\mu N \rightarrow \bar{\nu}_\mu X)}{\sigma(\bar{\nu}_\mu N \rightarrow \mu^+ X)} , \\ r &= \frac{\sigma(\bar{\nu}_\mu N \rightarrow \mu^+ X)}{\sigma(\nu_\mu N \rightarrow \mu^- X)} , \end{aligned} \quad (2.27)$$

are given by [21]

$$\begin{aligned} g_L^2 &= \rho_*(0)^2 \left[\frac{1}{2} - s_*^2(0) + \frac{5}{9} s_*^4(0) \right] , \\ g_R^2 &= \rho_*(0)^2 \left[\frac{5}{9} s_*^4(0) \right] . \end{aligned} \quad (2.28)$$

We can apply (2.25) and (2.10) to determine the influence of general oblique corrections on the value of these parameters.

We may summarize the results of this section as follows: The effects of oblique electroweak radiative corrections on weak-interaction observables may be computed

from the lowest-order expressions for these observables by replacing the bare parameters by the corresponding starred parameters of Kennedy and Lynn. The dependence of the starred functions on oblique corrections is relatively simple; it is expressed in Eqs. (2.10), (2.18), and (2.25). These relations may be reduced further by judicious approximations, and we will do this in the next section.

In the course of this section, we have given a few examples in which weak-interaction observables are expressed in terms of the starred parameters. For reference, we list in Appendix A a table of these relations for the most important observables of the current generation of weak-interaction experiments.

III. THE S, T, U PARAMETERS

As we have seen in the previous section, the effect of oblique corrections on weak-interaction observables can be summarized in the starred functions of Kennedy and Lynn. However, the formulas we write are not yet quite straightforward to apply, because even at lowest order, the formulas depend on three parameters e^2 , s^2 , and v^2 , that is, on the $SU(2) \times U(1)$ gauge couplings g and g' and the Higgs-boson vacuum expectation value. To make predictions based on the Kennedy-Lynn formalism, we must eliminate these three parameters in terms of three observables. If we were considering a theory without custodial symmetry, the lowest-order expressions would have contained ρ as a fourth parameter, and we would have needed a fourth observable to fix this variable. We will restrict ourselves to the three parameter case in the following.

The logical choice for the three input observables is α , G_F , and m_Z . They are the most accurately measured parameters of electroweak interactions and serve as excellent reference points. Their measured values are currently [22,23]

$$\begin{aligned} \alpha^{-1} &= 137.0359895(61) , \\ G_F &= 1.16637(2) \times 10^{-5} (\text{GeV})^{-2} , \\ m_Z &= 91.174(21) \text{ GeV} . \end{aligned} \quad (3.1)$$

It is convenient to represent this information as a value of the weak mixing angle. Here one must be a bit careful, since there are many ways of defining the weak mixing angle, and each of these appears as the favored definition in some paper in the literature. In general, we follow the usage of Ref. [4], which defines four versions of $\sin^2\theta_W$: the modified minimal subtraction ($\overline{\text{MS}}$) definition, which will not appear in this work; the Sirlin [24] definition, based on the values of m_W and m_Z ,

$$s_W^2 \equiv 1 - \frac{m_W^2}{m_Z^2} ; \quad (3.2)$$

a definition based on Z^0 asymmetries,

$$\bar{s}_W^2 \equiv s_*^2(m_Z^2) \quad (3.3)$$

(up to details of the treatment of box diagrams which are numerically unimportant at the Z^0); and a definition of s_0^2

based on α , G_F , and m_Z ;

$$\sin 2\theta_0 \equiv \left[\frac{4\pi\alpha_{*,0}(m_Z^2)}{\sqrt{2}G_F m_Z^2} \right]^{1/2}, \quad (3.4)$$

where

$$\alpha_{*,0}^{-1}(m_Z^2) = 128.80 \pm 0.12 \quad (3.5)$$

is the running electric charge evaluated at the Z^0 mass, with the running from $q^2=0$ to $q^2=m_Z^2$ calculated from known physics only [25]. The Sirlin definition is often called the ‘‘on-shell scheme,’’ though s_0^2 and \bar{s}_W^2 are also on-shell definitions.

These various versions of $\sin^2\theta_W$ are all equivalent at lowest order to the bare values s^2 , but they differ significantly from this value and from one another as a result of radiative corrections. Since s_0^2 requires only the values (3.1), (3.5), as inputs, it is extremely accurately known:

$$s_0^2 = 0.23146 \pm 0.00034. \quad (3.6)$$

Taking this value as a reference, we may predict the value of any other $\sin^2\theta_W$, or any other weak-interaction observable, in terms of radiative corrections.

We will now work out explicitly the part of that relation which is due to oblique corrections. To begin, we need the relation between s_0^2 and the bare value s^2 . This is found by using the identity

$$\begin{aligned} \delta(\sin^2\theta_W) &= 2sc\delta\theta_W = \frac{2sc}{2\cos 2\theta_W} \delta \sin 2\theta_W \\ &= \frac{2s^2c^2}{c^2-s^2} \frac{\delta \sin 2\theta_W}{\sin 2\theta_W}, \end{aligned} \quad (3.7)$$

where $s = \sin\theta_W$ and $c = \cos\theta_W$, together with the relations (2.10), (2.12), (2.25) which give the shifts of α , G_F , and m_Z due to oblique corrections. This gives

$$\begin{aligned} s_0^2 &= s^2 + \frac{2s^2c^2}{c^2-s^2} \cdot \frac{1}{2} \left[\frac{\delta\alpha_{*,0}}{\alpha_{*,0}} - \frac{\delta G_F}{G_F} - \frac{\delta m_Z^2}{m_Z^2} \right] \\ &= s^2 + \frac{s^2c^2}{c^2-s^2} \left[e^2\Pi'_{QQ}(0) + \frac{e^2}{s^2c^2m_Z^2}\Pi_{11}(0) - \frac{e^2}{s^2c^2m_Z^2}(\Pi_{33} - 2s^2\Pi_{3Q} + s^4\Pi_{QQ})(m_Z^2) \right], \end{aligned} \quad (3.8)$$

where we have included only oblique corrections due to new physics.

Combining (3.8) with (2.10) and (2.12), we find

$$\begin{aligned} \frac{m_W^2}{m_Z^2} - c_0^2 &= s_0^2 - s_W^2 \\ &= - \left[\frac{e^2c^2}{s^2(c^2-s^2)m_Z^2} \left[\Pi_{33}(m_Z^2) - 2s^2\Pi_{3Q}(m_Z^2) - \frac{s^2}{c^2}\Pi_{11}(0) - \frac{c^2-s^2}{c^2}\Pi_{11}(m_W^2) \right] \right. \\ &\quad \left. + \frac{e^2s^2c^2}{c^2-s^2} [\Pi'_{QQ}(m_Z^2) - \Pi'_{QQ}(0)] \right], \\ s_*^2(q^2) - s_0^2 &= \left[\frac{e^2}{c^2-s^2} \left[\frac{\Pi_{33}(m_Z^2) - 2s^2\Pi_{3Q}(m_Z^2) - \Pi_{11}(0)}{m_Z^2} - (c^2-s^2) \frac{\Pi_{3Q}(q^2)}{q^2} \right] \right. \\ &\quad \left. + \frac{e^2s^2}{c^2-s^2} [s^2\Pi'_{QQ}(m_Z^2) - c^2\Pi'_{QQ}(0) + (c^2-s^2)\Pi'_{QQ}(q^2)] \right]. \end{aligned} \quad (3.9)$$

The remaining starred functions are defined as deviations from 1, and so the formulas of Sec. II may be evaluated directly. From (2.25) and (2.18), we have

$$\begin{aligned} \rho_*(0) - 1 &= \frac{e^2}{s^2c^2m_Z^2} [\Pi_{11}(0) - \Pi_{33}(0)], \\ Z_{Z^*}(q^2) - 1 &= \frac{e^2}{s^2c^2} \left[\frac{d}{dq^2} (\Pi_{33} - 2s^2\Pi_{3Q} + s^4\Pi_{QQ}) \Big|_{q^2=m_Z^2} - (c^2-s^2)\Pi'_{3Q}(q^2) - s^4\Pi'_{QQ}(q^2) \right], \\ Z_{W^*}(q^2) - 1 &= \frac{e^2}{s^2} \left[\frac{d}{dq^2} \Pi_{11} \Big|_{q^2=m_W^2} - \Pi'_{3Q}(q^2) \right]. \end{aligned} \quad (3.10)$$

We note again that (3.9) and (3.10) present only the oblique corrections to the various starred parameters. The calculation of the full standard-model corrections is much more involved and cannot be expressed in such simple formulas. But it is remarkable that the entire influence of new physics, to the extent that it is purely oblique, follows from the relatively simple relations (3.9) and (3.10) and the use of the starred functions to renormalize the tree-level formulas. This point has, of course, been known for a long time; for example, it is the major result of Ref. [6].

If the physics included in the vacuum polarization diagrams is associated with new heavy particles of mass much larger than m_Z , the vacuum-polarization amplitudes will have rapidly convergent Taylor-series expansions in q^2 . Thus, it is natural to expand the various Π 's in q^2 and to neglect terms of order q^4 and above. This gives

$$\begin{aligned}\Pi_{\mathcal{Q}\mathcal{Q}}(q^2) &\approx q^2 \Pi'_{\mathcal{Q}\mathcal{Q}}(0), \\ \Pi_{3\mathcal{Q}}(q^2) &\approx q^2 \Pi'_{3\mathcal{Q}}(0), \\ \Pi_{33}(q^2) &\approx \Pi_{33}(0) + q^3 \Pi'_{33}(0), \\ \Pi_{11}(q^2) &\approx \Pi_{11}(0) + q^2 \Pi'_{11}(0).\end{aligned}\tag{3.11}$$

This approximation should only induce a relative error of (m_Z^2/m_T^2) , where m_T is the scale where the new physics resides.

When we insert the approximate formulas (3.11) into (3.9) and (3.10), three linear combinations of the six Taylor-series coefficients must cancel out, since these equations are differences of radiative corrections which fix α , G_F , and m_Z . These subtractions remove the ultraviolet divergences of perturbation theory, and so the three combinations which remain must be differences of coefficients with canceling ultraviolet divergences. It is natural to define these three ultraviolet-finite combinations of Taylor-series coefficients as new weak-interaction parameters [13,14]

$$\begin{aligned}\alpha S &\equiv 4e^2[\Pi'_{33}(0) - \Pi'_{3\mathcal{Q}}(0)], \\ \alpha T &\equiv \frac{e^2}{s^2 c^2 m_Z^2}[\Pi_{11}(0) - \Pi_{33}(0)], \\ \alpha U &\equiv 4e^2[\Pi'_{11}(0) - \Pi'_{33}(0)].\end{aligned}\tag{3.12}$$

Several different notations for these parameters appear in the literature; we review these notations and their interrelations in Appendix C.

We have already noted that, when the approximation (3.11) is inserted into (3.9) and (3.10), these formulas reduce to linear functions of S , T , and U . In fact, the relations are quite transparent:

$$\begin{aligned}\frac{m_W^2}{m_Z^2} - c_0^2 &= \frac{\alpha c^2}{c^2 - s^2} \left[-\frac{1}{2}S + c^2 T + \frac{c^2 - s^2}{4s^2} U \right], \\ s_*^2(q^2) - s_0^2 &= \frac{\alpha}{c^2 - s^2} (\frac{1}{4}S - s^2 c^2 T), \\ \rho_*(0) - 1 &= \alpha T, \\ Z_{Z^*}(q^2) - 1 &= \frac{\alpha}{4s^2 c^2} S, \\ Z_{W^*}(q^2) - 1 &= \frac{\alpha}{4s^2} (S + U).\end{aligned}\tag{3.13}$$

The error involved in the reduction from the original perturbative formulas to (3.13) is of order $\alpha(m_Z/m_T)^2$, where m_T is the scale of new physics. Subject to this uncertainty, the relations (3.13) contain the most general oblique correlations from new physics at very high energy.

It is a shame that (3.13) involves three new parameters, since it is easier to think about the relation of observables in a two-parameter space. However, the parameter U plays a fairly unimportant role. The functions $s_*^2(q^2)$, $\rho_*(q^2)$, and $Z_{Z^*}(q^2)$ have no dependence on U . This means that all neutral-current and low-energy observables depend only on S and T . In fact, the only accurately measured weak-interaction observable that depends on U is m_W . In addition, U is often predicted to be very small. We are already assuming that a custodial symmetry constrains the $\Pi_{11}(0)$ and $\Pi_{33}(0)$ to be equal to the level of order 1%, with the difference generated by radiative corrections. In most models, this approximate equality holds for all q^2 , so that U should differ from zero by only a percent of T . Altarelli and Barbieri [16] have pointed out that this argument does not apply to models with anomalous W interactions [26], so there is value in expressing constraints in the three-parameter space. However, we will often add to the assumptions above the further assumption that $U=0$ and project down to a two-dimensional parameter space in which the experimental constraints are easy to visualize.

In either its two- or three-parameter form, the set of relations (3.13) can be directly compared to observables of the weak interactions. To make this comparison, we simply use the formulas (3.13) to evaluate the shifts in the starred functions, then use the formulas of Appendix A to convert these to shifts of observables. Of course (3.13), contains only the influence of new physics and is not in any way a correct representation of the standard-model contributions. But these shifts are small and accurately represented. Thus, the relations (3.13) tell us what to add on to a highly accurate standard-model calculation to represent the effects of heavy physics. For example, from the first line of (3.13), we infer

$$\begin{aligned}m_W^2 &= m_W^2(\text{ref}) \\ &+ \frac{\alpha c^2}{c^2 - s^2} m_Z^2 \left[-\frac{1}{2}S + c^2 T + \frac{c^2 - s^2}{4s^2} U \right],\end{aligned}\tag{3.14}$$

where $m_W(\text{ref})$ is the value of m_W computed as accurately as possible in the standard model. We present the full

set of these relations for the most important weak-interaction observables in Appendix B.

A bit of further care is required to make relations of the form of (3.14) precise. The values of weak-interaction observables in the standard model depend on the unknown masses of the top quark and the Higgs boson. In order to specify properly the standard model from which S , T , and U parametrize the deviations, we must specify the values of m_t and m_H used in the standard-model computation. Thus, when we determine the constraints on S and T from the experimental data, we will specify that these refer to a specific set of reference values: $m_t = 150$ GeV, $m_H = 1$ TeV, in our analysis. (If the true values of m_t and m_H differ from these, the discrepancies will be approximately parametrized by shifts of S and T ; we will see how this works in Sec. IX.) Predictions for S and T from specific models of new physics may also depend on the reference point chosen, and this must be taken into account in comparing theory and experiment.

On the other hand, if the values of m_t and m_H were known, relation (3.14) and the other relations tabulated in Appendix B would be a set of direct relations between observable quantities in terms of the three parameters S , T , and U . The relations among the various formulas in Appendix B are the observable consequences of the assumption that new physics, beyond the standard model, is heavy and contributes obliquely. The final formulas are independent of any calculational scheme. It is this feature that motivated us to add the S and T parameters to the already lengthy and confusing list of notations for weak-interaction radiative corrections. Once one has understood the standard part of the calculation in one's own favorite notation, these parameters provide a representation of the discrepancies expected from nonstandard physics in a manner independent of the calculational conventions.

IV. S , T , AND U , IN PERTURBATION THEORY

The parameters S and T have one additional important property: They partition the contribution of electroweak radiative corrections into pieces with distinct physical significance. This separation is most clear in models where $U \approx 0$, so that a two-parameter representation applies. The parameter T obtains contributions only from effects which violate the custodial isospin symmetry. On the other hand, S is an isospin symmetric observable which measures the momentum dependence of Π_{33} (or, more properly, the ultraviolet-finite part of this dependence). In this section, we will see in several examples that S is a dimensionless measure of the size of the sector which contributes to Π_{33} .

The simplest example of oblique electroweak corrections are those due to new heavy fermions. As long as we can ignore small elements of the quark or lepton mixing matrices, the contributions of new fermions to electroweak processes appear via the simple one-loop diagrams shown in Fig. 2(a). For concreteness, we consider a fermion doublet (N, E) with the usual left-handed coupling to $SU(2)$, hypercharge Y , and masses m_N, m_E . It is straightforward to evaluate the vacuum-polarization diagrams which contribute to (3.12). In the limit

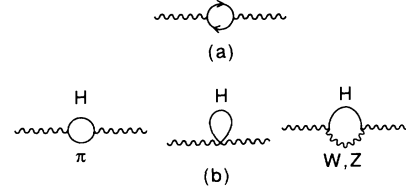


FIG. 2. Diagrams contributing to one-loop electroweak radiative corrections (a) due to a heavy fermion, (b) due to the standard-model Higgs boson.

$m_N, m_E \gg m_Z$, we find the contributions

$$\begin{aligned} S &= \frac{1}{6\pi} \left[1 - Y \ln \left[\frac{m_N^2}{m_E^2} \right] \right], \\ T &= \frac{1}{16\pi s^2 c^2 m_Z^2} \left[m_N^2 + m_E^2 - \frac{2m_N^2 m_E^2}{m_N^2 - m_E^2} \ln \left[\frac{m_N^2}{m_E^2} \right] \right], \\ U &= \frac{1}{6\pi} \left[-\frac{5m_N^4 - 22m_N^2 m_E^2 + 5m_E^4}{3(m_N^2 - m_E^2)^2} \right. \\ &\quad \left. + \frac{m_N^6 - 3m_N^4 m_E^2 - 3m_N^2 m_E^4 + m_E^6}{(m_N^2 - m_E^2)^3} \ln \left[\frac{m_N^2}{m_E^2} \right] \right]. \end{aligned} \quad (4.1)$$

The above expression for T is positive semidefinite [27] while those for S and U are not. However, if we assume that $\Delta m \equiv |m_N - m_E| \ll m_N, m_E$, we find

$$\begin{aligned} S &\approx \frac{1}{6\pi}, \\ T &\approx \frac{1}{12\pi s^2 c^2} \left[\frac{(\Delta m)^2}{m_Z^2} \right], \\ U &\approx \frac{2}{15\pi} \left[\frac{(\Delta m)^2}{m_N^2} \right]. \end{aligned} \quad (4.2)$$

This shows that S and U are also positive in the limit where the isospin breaking in the doublet is small. Also, as conjectured, U is suppressed compared to T by a factor of (m_Z^2/m_N^2) .

Note that each extra fermion doublet that we put into the theory will contribute additively to S and T . Therefore, S can be thought of as the measure of the total size of the new sector while T is the measure of the total weak-isospin breaking induced by it. The contribution $S \approx 1/6\pi$ is the origin of the additive effective of degenerate heavy generations on the W mass and the Z^0 polarization asymmetry, highlighted by Bertolini and Sirlin [28] and in Ref. [6].

As another example of the evaluation of S , T , and U , let us consider the contribution of the Higgs boson. Though the Higgs boson does not exactly qualify as belonging to physics beyond the standard model, it is true that the only one-loop diagrams which depend on the Higgs-boson mass are the oblique corrections shown in Fig. 2(b). When the mass of the Higgs boson is very large compared to m_Z , these contributions should be well represented by S , T , and U . Keeping only the leading

logarithms in the Higgs-boson mass, we find

$$\begin{aligned} S &\approx \frac{1}{12\pi} \ln \left[\frac{m_H^2}{m_{H,\text{ref}}^2} \right], \\ T &\approx -\frac{3}{16\pi c^2} \ln \left[\frac{m_H^2}{m_{H,\text{ref}}^2} \right], \\ U &\approx 0, \end{aligned} \quad (4.3)$$

where $m_{H,\text{ref}}$ is the reference value of the Higgs-boson mass from which S , T , and U are defined. Note that U is small compared to S and T for this case as well.

As a third and final example, we consider the contribution of the t quark. Again, as was the case with the Higgs boson, discussing the t -quark contribution in terms of S , T , and U is only strictly correct when $m_Z \ll m_t$. Also, unlike the Higgs boson, nonoblique t -quark corrections cannot be neglected when the external fermion is a b quark; this affects the prediction for $\Gamma(Z^0 \rightarrow b\bar{b})$. With these caveats in mind, we can compute the top-quark contribution to S , T , and U by evaluating (4.1) in the limit $m_E \rightarrow 0$, with an additional factor of 3 to account for color. We obtain

$$\begin{aligned} S &\approx -\frac{1}{6\pi} \ln \left[\frac{m_t^2}{m_{t,\text{ref}}^2} \right], \\ T &\approx \frac{3}{16\pi s^2 c^2} \left[\frac{m_t^2 - m_{t,\text{ref}}^2}{m_Z^2} \right], \\ U &\approx \frac{1}{2\pi} \ln \left[\frac{m_t^2}{m_{t,\text{ref}}^2} \right], \end{aligned} \quad (4.4)$$

where $m_{t,\text{ref}}$ is the reference value of the t -quark mass used in defining the S and T parameters. Again, we find U to be much smaller than T . In this case, S is small also, so that the major effect of a shift of m_t is just a shift of T .

For contributions to the electroweak vacuum polarizations from new heavy particles, the relations (4.2) give a good idea of the generic situation. The contributions to T are proportional to isospin-violating mass differences. On the other hand, S receives isospin-independent contributions which grow systematically with the size of the new sector. In the next few sections, we will argue that these properties of S and T also hold when the new physics is essentially nonperturbative.

V. A DISPERSIVE REPRESENTATION OF S

Let us now consider how we would calculate the values of the parameters of oblique corrections for theories in which the relevant vacuum-polarization diagrams cannot be computed by perturbation theory. The most important examples of such theories are models of technicolor, in which the Higgs sector is a strongly interacting gauge theory with a characteristic scale near 1 TeV. As they are usually constructed, technicolor theories have a custodial SU(2) symmetry, the isospin symmetry of the technicolor strong interactions, which protects the relation (1.1) from receiving large radiative corrections. Addi-

tional interactions, called extended technicolor, must break this symmetry to generate the observed isospin asymmetry in the quark and lepton mass spectrum; in general, then, these additional interactions will contribute to T and U . However, since the isospin-violating effect on the vacuum polarization must be small, the effect on the U parameter is doubly suppressed: $U \sim T(m_Z^2/m_T^2)$, where m_T is the technicolor mass scale. Thus, quite generally in technicolor theories, we can ignore U and adopt a two-parameter (S, T) description of oblique corrections.

By distinguishing in this way between the effects of technicolor and extended technicolor, we also clarify the separate significance of S and T in these technicolor models. Contributions to T are generated by extended technicolor. These corrections are large and troublesome, but they are difficult to estimate precisely and also strongly dependent on the detailed implementation of extended technicolor. (We will review various estimates of T in Sec. VIII.) The contributions to T thus resemble the other prominent experimental constraints on technicolor, such as the absence of light charged scalar particles and flavor-changing neutral currents: In the simplest models, they are severe restrictions on the theory, but one can reinterpret the problem as a constraint on the specific structure of the extended technicolor couplings.

On the other hand, the basic idea of technicolor, that the weak interactions are broken by dynamical chiral-symmetry breaking due to a new set of strong interactions, is a very attractive one. It would be wonderful if we could test this idea directly without needing to analyze a highly embellished model. The parameter S gives just such a test. In technicolor models, S receives contributions from the largest effects in the new strong-interaction sector. These effects are independent of isospin or flavor violation. Thus, to the extent that we can obtain a bound on S independently of T , this bound constrains the basic idea that the Higgs sector is built from a strongly interacting gauge theory.

In this section, we will set up a formalism for computing S in technicolor and related models in which the Higgs sector is strongly interacting. Our strategy will be to write a representation for S as a dispersive integral over the technicolor mass spectrum. In this analysis, we will make the assumption that the technicolor interactions have an exact isospin symmetry. For simplicity, we will also assume that the technicolor sector conserves parity; this is a property of most technicolor models.

To begin, we rewrite the electromagnetic and the left-handed isospin currents in terms of the (conventional) hypercharge current and the isospin vector and axial-vector currents:

$$J_3^\mu = \frac{1}{2}(J_V^\mu - J_A^\mu), \quad J_Q^\mu = J_V^\mu + \frac{1}{2}J_Y^\mu. \quad (5.1)$$

By our assumption that technicolor interactions conserve isospin and parity, we find

$$\Pi_{33} = \frac{1}{4}(\Pi_{VV} + \Pi_{AA}), \quad \Pi_{3Q} = \frac{1}{2}\Pi_{VV}, \quad (5.2)$$

where the Π 's on the right-hand side are the correlators of isospin vector and axial-vector currents. Since the vector symmetries are exact, while the axial-vector symmetries are spontaneously broken,

$$\begin{aligned}\Pi_{VV}(q^2) &= q^2 \Pi'_{VV}(q^2), \\ \Pi_{AA}(q^2) &= \Pi_{AA}(0) + q^2 \Pi'_{AA}(q^2) \\ &= F_\pi^2 + q^2 \Pi'_{AA}(q^2),\end{aligned}\quad (5.3)$$

where $F_\pi = 250$ GeV is the technipion decay constant, which is identified in technicolor models with the parameter v in (2.4). In terms of Π_{VV} and Π_{AA} we find

$$S = -4\pi[\Pi'_{VV}(0) - \Pi'_{AA}(0)]. \quad (5.4)$$

The vacuum polarizations in (5.4) are expectation values in a strong-interaction theory and cannot be computed by perturbation theory. The problem is quite similar to another problem in precision electroweak theory, that of computing the electromagnetic vacuum polarization due to the familiar strong interactions, to compute the renormalization of α . This latter problem was solved by using a dispersion relation to connect $\Pi'_{QQ}(q^2)$ to the measured quantity $R(s)$, the ratio of the cross sections for e^+e^- annihilation to hadrons and to $\mu^+\mu^-$ [29]. Since

$$\begin{aligned}R(s) &= \left[\frac{3s}{4\pi\alpha^2} \right] \sigma(e^+e^- \rightarrow \gamma \rightarrow \text{hadrons}) \\ &= -12\pi \text{Im}\Pi'_{QQ}(s)\end{aligned}\quad (5.5)$$

we have the relation

$$\begin{aligned}\Pi'_{QQ}(q^2) - \Pi'_{QQ}(0) &= -\frac{1}{12\pi} \int_0^\infty \frac{ds}{\pi} \left[\frac{1}{s-q^2} - \frac{1}{s} \right] R(s) \\ &= -\frac{q^2}{12\pi} \int_0^\infty \frac{ds}{\pi} \frac{R(s)}{s(s-q^2)}.\end{aligned}\quad (5.6)$$

The integral in (5.6) can be evaluated directly from the e^+e^- data.

A similar method can be used to estimate (5.4). Define vector and axial isospin analogues of $R(s)$ by

$$\begin{aligned}R_V(s) &\equiv -12\pi \text{Im}\Pi'_{VV}(s), \\ R_A(s) &\equiv -12\pi \text{Im}\Pi'_{AA}(s).\end{aligned}\quad (5.7)$$

These quantities would give the normalized e^+e^- total cross sections for a photon coupled to vector or axial isospin rather than electric charge. Of course, $R_V(s)$ and $R_A(s)$ are not measured for any technicolor theory, but we can infer many of their properties from our general knowledge of gauge theories. For example, as $s \rightarrow \infty$, R_V and R_A both approach the sum of the squares of the technifermion isospins, and thus also become asymptotically equal. On the other hand, at small s , $R_V(s)$ gets a contribution only from $\pi^+\pi^-$ production. For $m_\pi = 0$, $R_V(s) \rightarrow 1/4$ as $s \rightarrow 0$. $R_A(s)$ gets its first contribution from three-pion production, and so vanishes proportionally to s as $s \rightarrow 0$. At intermediate values of s , R_V , and R_A should have peaks at the vector and axial-vector resonances of the technicolor sector.

Using (5.7) and (5.3), we may write the dispersion relation

$$\begin{aligned}\Pi_{VV}(q^2) - \Pi_{AA}(q^2) &= q^2[\Pi'_{VV}(q^2) - \Pi'_{AA}(q^2)] - \Pi_{AA}(0) \\ &= -\frac{q^2}{12\pi} \int_0^\infty \frac{ds}{\pi} \frac{R_V(s) - R_A(s)}{s - q^2} - F_\pi^2.\end{aligned}\quad (5.8)$$

This equation gives some further properties of R_V and R_A . In asymptotically free gauge theories, one may show that the left-hand side of (5.8) is of order $1/q^4$ as $q^2 \rightarrow \infty$ [30]. Thus, the first two terms in the expansion of (5.8) for large q^2 give the following identities, called the first and second Weinberg rules [31]:

$$\begin{aligned}\frac{1}{3\pi} \int_0^\infty ds [R_V(s) - R_A(s)] &= 4\pi F_\pi^2, \\ \frac{1}{3\pi} \int_0^\infty ds s [R_V(s) - R_A(s)] &= 0.\end{aligned}\quad (5.9)$$

It is likely that at least the first of these sum rules is also true in gauge theories with nontrivial ultraviolet fixed points [32].

Taking the $q^2 \rightarrow 0$ limit of (5.8), we can evaluate the formula for S given in (5.4). This gives the following, still preliminary, result:

$$S = \frac{1}{3\pi} \int_0^\infty \frac{ds}{s} [R_V(s) - R_A(s)]. \quad (5.10)$$

Thus S is a ‘‘zerth Weinberg sum rule’’ of the strongly interacting Higgs sector. We can estimate S by making a reasonable model of the spectral functions R_V and R_A , consistent with the general constraints given above, and then using this model to evaluate (5.10). We will describe such an evaluation in Sec. VII.

Before attempting to estimate (5.10), however, we should point out two unsatisfactory aspects of this formula and repair them. First, we noted above that $R_V(s) \rightarrow 1/4$ while $R_A(s) \rightarrow 0$ as $s \rightarrow 0$. Thus, the integral in (5.10) is divergent at the lower limit. (The Weinberg sum rules imply that it is quite convergent as $s \rightarrow \infty$). Second, we defined S as a difference between the vacuum-polarization effects in a new theory and those in the standard model. If we are using the technicolor strong interactions to break $SU(2)_L \times U(1)_Y$, the standard Higgs sector is superfluous and we should subtract its contribution from the one-loop diagrams.

Fortunately, these two difficulties cancel one another. This is most easily seen by working in the Landau gauge. In this gauge, one must include, in addition to the physical Higgs boson, the unphysical Goldstone bosons which are absorbed into the W^+ , W^- , and Z^0 in the Higgs mechanism. In the Landau gauge, these Goldstone bosons are massless. We may neglect their coupling to external fermions, since this is proportional to the fermion mass. Thus, at one-loop order, these particles contribute only to vacuum-polarization diagrams; their contribution to S comes only from the diagrams shown in Fig. 3. These diagrams are easily evaluated and subtracted. The diagram with a two-Goldstone-boson intermediate state gives a contribution to the dispersion relation identical to the contribution from the two-pion state. When we subtract this contribution from (5.10), the in-

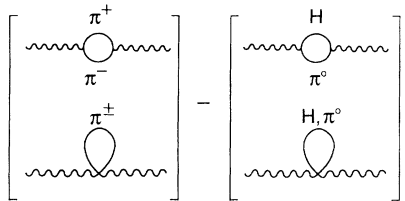


FIG. 3. The one-loop diagrams involving Higgs particles, which contribute to S in Landau gauge.

frared divergence in (5.10) cancels and we are left with a well-defined formula.

Explicitly subtracting the diagrams of Fig. 3 from (5.10), we find the final dispersion formula:

$$S = \frac{1}{3\pi} \int_0^\infty \frac{ds}{s} \left\{ [R_V(s) - R_A(s)] - \frac{1}{4} \left[1 - \left[1 - \frac{m_H^2}{s} \right]^3 \theta(s - m_H^2) \right] \right\}. \quad (5.11)$$

Notice that this formula depends on m_H , the mass of the physical Higgs boson in the standard-model calculation taken as a reference point in defining S . In our evaluation of S , we will take $m_H = 1$ TeV; one should take care to use the same reference point in deriving predictions for weak-interaction experiments.

We conclude this section by describing the relation between the parameter S as we have defined it and the parameters of chiral perturbation theory. Several of the early papers [5,6,8] attempted to estimate the electroweak radiative corrections from technicolor from the leading logarithms of chiral perturbation theory. However, the constant terms of the same order in derivatives are often equally or more important, and this should properly be taken into account. In their classic paper on renormalized chiral perturbation theory, Gasser and Leutwyler [33] discussed the sum rule (5.10) in a theory with nonzero pion mass and gave the following expression for it in terms of renormalized parameters:

$$\frac{1}{3\pi} \int_0^\infty \frac{ds}{s} [R_V(s) - R_A(s)] = \frac{1}{12\pi} (\bar{I}_5 - 1). \quad (5.12)$$

The integral is infrared finite because of the assumed nonzero value of m_π . The infrared logarithm is absorbed into the parameter \bar{I}_5 . To extract this dependence, define

$$\bar{I}_5(\mu) = \bar{I}_5 + \ln(m_\pi^2/\mu^2). \quad (5.13)$$

Then $\bar{I}_5(\mu)$ gives the high-mass contribution to the sum rule, and we have separated out the leading chiral logarithm. To relate this expression to S , one should modify the standard-model subtraction terms in (5.11) to include the Goldstone-boson mass m_π , carry out the integral over these terms, subtract the result from (5.12), and then take the limit $m_\pi \rightarrow 0$. This gives

$$S = \frac{1}{12\pi} \left[\bar{I}_5(\mu) + \ln \frac{\mu^2}{m_H^2} - \frac{1}{6} \right]. \quad (5.14)$$

This reproduces (with a slightly more careful evaluation) the computation of the technicolor electroweak correction in Refs. [9,11]. The value of $\bar{I}_5(\mu)$ is known in the familiar case of two flavors and three colors from the work of Gasser and Leutwyler; however, in more general situations, one needs a method of estimating this parameter. This leads us back to the dispersive formula (5.11). We will illustrate the use of this formula in Sec. VII.

VI. GAUGE INVARIANCE OF THE DISPERSIVE INTEGRAL

At this point, it would be natural to present numerical estimates for S based on the integral representation (5.11) derived in the previous section. However, in this section, we will pause to settle a lingering theoretical issue. The derivation of (5.11) that we gave in the previous section made essential use of the Landau gauge. We should, then, discuss to what extent (5.11) can be considered a gauge-invariant result. Our discussion will be somewhat formal. To simplify our notation, we will ignore the hypercharge gauge boson and consider a pure SU(2) weak-interaction theory.

Before beginning this discussion, we would like to describe a bit more clearly the question we wish to address. Weak-coupling perturbation theory in the standard model usually relies on the R_ξ gauges, which are defined by a gauge-fixing term of the form

$$\frac{1}{2\xi} (\partial^\mu W_\mu^a - \xi m_W \pi^a)^2, \quad (6.1)$$

where W_μ^a are the gauge fields, π^a are the Goldstone-boson fields, and ξ is an arbitrary gauge parameter. In this class of gauges, the Goldstone-boson fields have a gauge-dependent mass equal to $\sqrt{\xi} m_W$. The inclusion of this mass would distort the dispersive integral (5.11) in a gauge-dependent way. In fact, in the minimal version of the standard model, the ξ independence of fermion-fermion scattering amplitudes follows from series of subtle cancellations involving the Higgs- and gauge-boson two-point functions, the gauge-boson-fermion vertices, and the box diagrams. In a model in which the gauge symmetry is broken dynamically and the Goldstone bosons are composite, it is not clear whether it is convenient or useful or even possible to define an analogue of the R_ξ gauges. But the properties of these gauges in the minimal version of the standard model cast doubt on any claim that a pure self-energy calculation such as (5.11) has gauge-invariant significance. Let us now address and answer this question.

The Lagrangian of a general weak-interaction theory may be written in the form

$$\mathcal{L} = -\frac{1}{4} (F_{\mu\nu}^a)^2 + \mathcal{L}_f + \mathcal{L}_H, \quad (6.2)$$

where $F_{\mu\nu}^a$ is built from SU(2) gauge fields W_μ^a , \mathcal{L}_f is the Lagrangian governing the coupling of fermions to the W bosons, and \mathcal{L}_H is the Lagrangian of the Higgs sector. In principle, this last piece of the Lagrangian may contain the interactions of any other heavy particles. We will make three assumptions about the nature of \mathcal{L}_H : (1) \mathcal{L}_H

is a self-contained quantum field theory with a global SU(2) symmetry which is gauged by the W bosons; (2) \mathcal{L}_H spontaneously breaks this SU(2) symmetry; (3) \mathcal{L}_H predicts no massless particles except the SU(2) Goldstone bosons. In the spirit of the previous sections, we might wish to add a fourth assumption of obliqueness: (4) \mathcal{L}_H does not contain any terms involving light fermions. What we do not assume about \mathcal{L}_H is whether it is weakly interacting (e.g., standard model) or strongly interacting (e.g., technicolor). If it is weakly interacting, the Goldstone bosons will be elementary and will have corresponding Goldstone-boson “fields” in \mathcal{L}_H . If it is strongly interacting, the Goldstone bosons will be composite and their existence cannot be seen until the complete dynamics of \mathcal{L}_H has been worked out.

Because the theory \mathcal{L}_H is well defined in its own right, we can integrate it out, producing an effective Lagrangian with nonlocal vertices for the fermions and gauge bosons. In this procedure, we consider the W_μ^a fields as external classical sources acting on the \mathcal{L}_H field theory. The W fields then acquire new vertices corresponding to the connected multicurrent amplitudes of the \mathcal{L}_H theory. To be more explicit, let $\Gamma_H[W_\mu^a]$ be the effective action of the \mathcal{L}_H theory:

$$\Gamma_H[W_\mu^a] = -i \ln \left[\int \mathcal{D}\Phi \exp \left[i \int d^4x \mathcal{L}_H[\Phi, W_\mu^a] \right] \right], \quad (6.3)$$

where Φ is a generic expression for the dynamical fields of the \mathcal{L}_H theory. Integration over Φ produces an effective action for the W bosons and fermions:

$$S = \int d^4x \left[-\frac{1}{4}(F_{\mu\nu}^a)^2 + \mathcal{L}_f \right] + \Gamma_H[W_\mu^a]. \quad (6.4)$$

The last term of (6.4) modifies the W propagator and produces new vertices proportional to the successive functional derivatives of Γ_H with respect to $W_\mu^a(x)$. These are the connected correlation functions of the pure Higgs theory. In particular, the two-point function

$$i \left[g^{\mu\nu} - \frac{q^\mu q^\nu}{q^2} \right] \Pi_H(q^2) \equiv \int d^4x e^{-iqx} \frac{\delta^2}{\delta W_\mu^a(x) \delta W_\nu^b(0)} \Gamma_H \quad (6.5)$$

will have the Goldstone pole required by our assumption (2):

$$\Pi_H(q^2) = \frac{g^2 F_\pi^2}{4} + q^2 \Pi'_H(q^2). \quad (6.6)$$

Notice that, from our assumptions (1)–(3) above, the vertices of Γ_H are well defined and SU(2) symmetric. As a result, the complete effective action is invariant under local SU(2) gauge transformations. It is also important to note that, since \mathcal{L}_H is a globally symmetric theory coupled to external gauge bosons, the transition from (6.2) to (6.4) requires no gauge fixing. This procedure of integrating out the Higgs sector can be applied to both weakly interacting and strongly interacting Higgs sector theories.

Let us now modify the action (6.4) by introducing a parameter λ as

$$S_\lambda = \frac{1}{\lambda} S. \quad (6.7)$$

We may now compute amplitudes governed by the action S_λ as a perturbation series in λ . At this stage of the calculation, we must introduce a gauge-fixing term and a Faddeev-Popov determinant. However, λ has been defined before gauge fixing, and so physical quantities computed from this action will be gauge invariant order by order in λ . This situation is analogous to the usual perturbation expansion in \hbar .

To carry out the λ expansion explicitly, we must choose a gauge. Note that the usual R_ξ gauges cannot be used here. The Goldstone boson fields which appear in (6.1) have already been integrated out. Also, if the Higgs sector had been strongly interacting, there would have been no Goldstone boson “fields” to begin with. We should therefore consider adding a gauge-fixing term which involves only the unintegrated fields; for example,

$$\frac{1}{2\xi} (\partial^\mu W_\mu^a)^2. \quad (6.8)$$

We may then display the λ perturbation theory diagrammatically. We will represent the vertices following from Γ_H , that is, the functional derivatives of Γ_H , as shaded blobs, as shown in Fig. 4. To these must be added the usual three- W and four- W vertices coming from the $(F_{\mu\nu}^a)^2$ term. We represent the sum of the elementary Yang-Mills and Higgs-induced vertices by unshaded blobs, as shown in Fig. 5(a). When the gauge-fixing term (6.8) is used, the W propagator in the λ expansion is given by

$$-i \left[\frac{g^{\mu\nu} - q^\mu q^\nu / q^2}{q^2 - \frac{1}{4} g^2 F_\pi^2 - q^2 \Pi'_H(q^2)} + \xi \frac{q^\mu q^\nu}{(q^2)^2} \right]; \quad (6.9)$$

this expression represents the sum of diagrams shown in Fig. 5(b). We represent this propagator with a wavy line with an unshaded blob on it.

Using these diagrammatical notations, we find that the tree and one-loop order contributions (in the λ expansion) to fermion-fermion scattering are those shown in Fig. 6. We emphasize here again that this expansion is gauge invariant order by order since S_λ is gauge invariant.

The tree diagram of the λ expansion already includes infinite orders of the \hbar expansion through F_π and $\Pi'_H(q^2)$ in the W propagator. Comparing (6.9) with the usual W propagator of the \hbar expansion, we see that $\Pi'_H(q^2)$ includes precisely the oblique corrections we were consider-

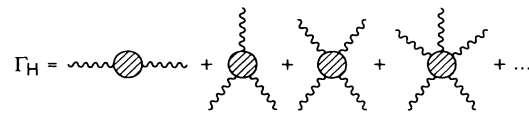


FIG. 4. Diagrammatic expansion of the effective action Γ_H . The shaded blobs are connected multi- W amplitudes computed from the Lagrangian \mathcal{L}_H .

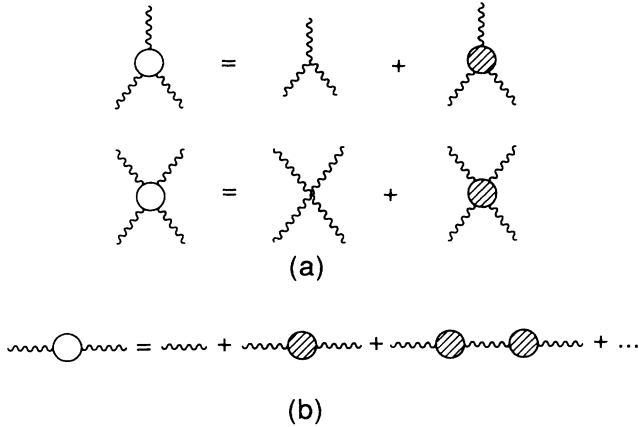


FIG. 5. Ingredients of the λ expansion: (a) the 3- W and 4- W vertices, constructed from the gauge Lagrangian and the effective action Γ_H ; (b) the W propagator.

ing in the previous sections. Indeed,

$$\Pi'_H(q^2) = \frac{g^2}{4} [\Pi'_{VV}(q^2) + \Pi'_{AA}(q^2)]. \quad (6.10)$$

Thus, our whole formula for the oblique correction due to the Higgs sector, including the specific piece (5.10) contributing to S , is gauge invariant in the class of gauges for which the λ expansion makes sense.

However, even though our expression for (5.10) is gauge invariant, we must worry that it is not infrared regular. In fact, we encountered massless Goldstone modes when we integrated out the Higgs sector to derive (6.4); also, in the gauges (6.8), unlike the usual R_ξ gauges, the W propagator contains massless poles. As a result, quantities such as $\Pi'_H(q^2)$ diverge logarithmically as $q^2 \rightarrow 0$. To cure this problem, we can apply in a quite general way the method used at the end of the previous section: Go back to the generating functional with action (6.2), and multiply and divide by the functional integral over Higgs

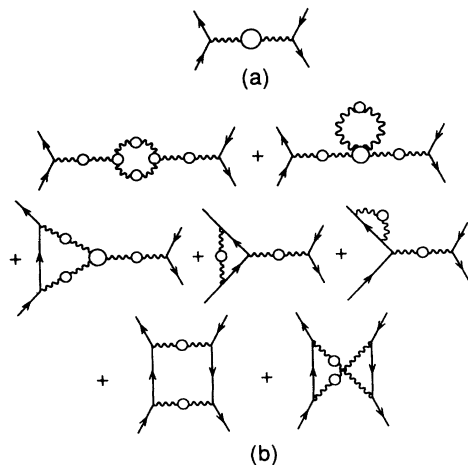


FIG. 6. Diagrams contributing to fermion-fermion scattering in the λ expansion (a) at tree level; (b) at one-loop order.

fields of the exponential of the standard-model Higgs Lagrangian \mathcal{L}_H^0 . Performing one of these functional integrations, we find an effective action of the form

$$S = \int d^4x \left[-\frac{1}{4}(F_{\mu\nu}^a)^2 + \mathcal{L}_f + \mathcal{L}_H^0 \right] + (\Gamma_H[W_\mu^a] - \Gamma_H^0[W_\mu^a]). \quad (6.11)$$

Since the leading infrared singularities of Γ_H are associated with soft pions, they are determined by chiral symmetry and so are identical, and canceling, between Γ_H and Γ_H^0 . If we now carry out the λ expansion by taking the term in parentheses in (6.11) as the perturbation, we find a formula for the oblique corrections which implies our final, subtracted formula (5.11). This derivation clarifies that this formula is both gauge invariant and infrared finite.

Another point of view on this question has been emphasized to us by Golden and Randall [34]. They point out that the parameters of the chiral effective Lagrangian, such as \bar{I}_5 in (5.14), are gauge invariant. Our formalism can be thought of as giving a relation between this unambiguously defined parameter of the new strong interactions and observable parameters of the weak interactions.

VII. ESTIMATION OF S

Now that we have clarified the theoretical foundation of the integral formula (5.11), let us put this formula to use by estimating the value of S in a number of technicolor models. Estimates of S in technicolor theories requires nontrivial information about the technicolor strong interactions. Since no exact solution of strongly interacting gauge theories is available, such estimates will depend on the model assumptions used to treat the strong interactions.

In our earlier paper, Ref. [13], we gave an estimate for S based on scaling up the strong-interaction data on the e^+e^- total cross section to hadrons. In the literature, a variety of other techniques have been used to estimate the radiative corrections due to technicolor, including computations based on vector-meson dominance and chiral perturbation theory. Some of these models have been assembled and compared by Cahn and Suzuki [35]. In this section, we will review these simpler methods of estimation, then present an improved version of our calculation of S , and finally assemble all of this information to determine the approximate value of S and its uncertainty.

The simplest model for $R_V(s)$ and $R_A(s)$ is the vector-dominance model in which we saturate each of $R_V(s)$ and $R_A(s)$ with a single vector-meson pole:

$$\begin{aligned} R_V(s) &= 12\pi^2 F_{\rho_T}^2 \delta(s - m_{\rho_T}^2), \\ R_A(s) &= 12\pi^2 F_{a_{1T}}^2 \delta(s - m_{a_{1T}}^2), \end{aligned} \quad (7.1)$$

where m_{ρ_T} and $m_{a_{1T}}$ are the techni- ρ and techni- a_1 masses, respectively. As Weinberg observed in his original paper, the parameters of (7.1) are constrained by the first and second Weinberg sum rules [31]:

$$\begin{aligned} \int ds [R_V(s) - R_A(s)] &= 12\pi^2 F_\pi^2, \\ \int ds s [R_V(s) - R_A(s)] &= 0, \end{aligned} \quad (7.2)$$

where $F_\pi = 250$ GeV is the technipion decay constant; we find

$$F_{\rho_T}^2 = \frac{m_{a_{1T}}^2 F_\pi^2}{m_{a_{1T}}^2 - m_{\rho_T}^2}, \quad F_{a_{1T}}^2 = \frac{m_{\rho_T}^2 F_\pi^2}{m_{a_{1T}}^2 - m_{\rho_T}^2}. \quad (7.3)$$

This gives

$$\begin{aligned} S &= \frac{1}{3\pi} \int \frac{ds}{s} [R_V(s) - R_A(s)] \\ &= 4\pi \left[1 + \frac{m_{\rho_T}^2}{m_{a_{1T}}^2} \right] \frac{F_\pi^2}{m_{\rho_T}^2}. \end{aligned} \quad (7.4)$$

Assuming the large- N rescaling relations between the technisector and QCD [37],

$$\frac{m_{\rho_T}^2}{m_{a_{1T}}^2} = \frac{m_\rho^2}{m_{a_1}^2}, \quad \frac{F_\pi^2}{m_{\rho_T}^2} = \frac{N_{\text{TF}}}{2} \frac{N_{\text{TC}}}{3} \frac{f_\pi^2}{m_\rho^2}, \quad (7.5)$$

with $f_\pi = 93$ MeV, $m_\rho = 770$ MeV, and $m_{a_1} = 1260$ MeV, we find

$$S \approx 0.25 \frac{N_{\text{TF}}}{2} \frac{N_{\text{TC}}}{3}, \quad (7.6)$$

where N_{TF} and N_{TC} are the numbers of techniflavors and technicolors, respectively. Note that, in this estimate, the integral under the ρ contributes 0.29 to the prefactor, and so that the a_1 gives a relatively small subtraction.

A second simple model for R_V and R_A is that of keeping only the leading logarithms of chiral perturbation theory. In this approximation, we replace R_V by the contribution of pseudo Goldstone bosons (cut off at the same of hadronic resonances, e.g., at m_{ρ_T}) and ignore altogether the higher-mass intermediate states which contribute to R_A . In a model with N_{TF} flavors, there are $(N_{\text{TF}}/2)^2$ pairs of pseudo Goldstone bosons with $I^3 = \pm 1$. Each pair contributes $\frac{1}{4}$ to R_V . Let us remove the true Goldstone bosons [which are subtracted in (5.11)], and assign the remaining pseudo Goldstone bosons an averaged mass m_p . Then this approximation gives

$$S \approx \frac{1}{12\pi} \left[\frac{N_{\text{TF}}^2}{4} - 1 \right] \ln \frac{m_{\rho_T}^2}{m_p^2}. \quad (7.7)$$

In a minimal technicolor model with $N_{\text{TF}} = 2$, this approximation give no contribution to S . However, in a model with $N_{\text{TF}} = 8$, one generation of technifermions, and the values $m_{\rho_T} = 900$ GeV, $m_p = 200$ GeV, in the logarithm, we find a quite substantial contribution:

$$S \approx 1.2. \quad (7.8)$$

The estimate (7.8) is consistent with (7.6), but this consistency is misleading. The formulas (7.6) and (7.7) have a completely different dependence on N_{TF} and N_{TC} [35]. This difference reflects the fact that the two formulas are

based on completely different physics. In particular, (7.7) knows nothing about the strength of the ρ resonance, which gives the major contribution to (7.6). Thus, one cannot obtain a reasonable estimate of the value of S in a particular technicolor theory by simple scaling, either from (7.6) or from (7.7). One needs a more sophisticated approach, which takes into account the fact that the contributions to S from different intermediate states have a different dependence on N_{TF} and N_{TC} and merges these dependences into a coherent picture of the spectrum of technicolor states in the vector and axial-vector channels.

We have attempted to construct such a picture based on the general notion that technicolor dynamics is a scaled-up version of the familiar strong interactions. Our strategy is to write a parametric formula for R_V and R_A which is a reasonable representation of the data from the familiar strong interactions. We then assign each piece of this formula its own characteristic dependence on N_{TF} and N_{TC} . For each value of these parameters, we obtain a distorted spectral function which we can then integrate to find the corresponding value of S .

Much of the recent work on technicolor models has centered on the idea that technicolor dynamics is not simply a scaled-up version of the familiar strong interactions, but rather has a very different high-energy behavior. On the other hand, Cahn and Suzuki [36,35] have argued that the technicolor strong interactions may also be different at low energies, if the shape of the techni- ρ resonance is distorted by the coupling of the techni- ρ to pseudo Goldstone bosons. Our analysis takes a much more conservative picture of the strong technicolor interactions. However, we believe that it can be useful in addressing the effect of a modification of the technicolor theory, by indicating in one concrete scheme the fraction of the final value of S which comes from the affected momentum region. This allows one to estimate the uncertainty in S that would result from a possible distortion of the technicolor spectrum in this region.

We now present the details of our estimate. The first step is to obtain functional descriptions of the values of R_V and R_A in the familiar strong interactions. For QCD, $R_V(s)$ can be extracted from the data on

$$R(s) = \frac{\sigma(e^+e^- \rightarrow \text{hadrons})}{\sigma(e^+e^- \rightarrow \mu^+\mu^-)}. \quad (7.9)$$

This is because $R(s)$ is the imaginary part of Π'_{QQ} while $R_V(s)$ is the imaginary part of Π'_{VV} and they are related by

$$\Pi'_{QQ} = \Pi'_{VV} + \frac{1}{4}\Pi'_{YY}. \quad (7.10)$$

Below roughly 3 GeV, only the u , d , and s quarks are light enough to be pair created so the final hadronic products of e^+e^- annihilation will consist of pions and kaons. By looking at events in which only pions are produced we can effectively eliminate any s -quark contribution to $R(s)$. The remaining pure pion events will be partially $I=0$ and partially $I=1$. Because e^+e^- annihilation into hadrons goes through a vector current, the resulting hadronic state will have $C = -1$. This means that the $I=0$ states will have G parity $G = C(-1)^I = -1$

while the $I=1$ states will have G parity $G=+1$. A pion's G parity is -1 so the $G=-1$ states can only decay into an odd number of pions while the $G=+1$ states can only decay into an even number of pions. Therefore, looking at only the even pion production events will give us $R_V(s)$.

On the other hand, $R_A(s)$ for QCD can be extracted from the data on τ decay into a τ neutrino and hadrons. This decay goes through a virtual W so it measures the imaginary part of

$$\Pi'_{11} = \frac{1}{4}(\Pi'_{VV} + \Pi'_{AA}). \quad (7.11)$$

The Π'_{VV} and Π'_{AA} appearing on the right-hand side are charged-current objects but they are equal to their neutral-current counterparts because of isospin invariance. This time, the virtual W only couples to $I=1$ states. Therefore, states produced by the vector current will have $C=-1$ and $G=+1$, and the states produced by the axial-vector current will have $C=+1$ and $G=-1$. Again, the conservation of G parity tells us that the vector states only decay into an even number of pions while the axial-vector states only decay into an odd number of pions. Looking at odd pion decays will give us $R_A(s)$. Unfortunately, τ decay can only tell us what $R_A(s)$ is up to the τ mass. The behavior of $R_A(s)$ above that energy must be deduced by other means.

The analysis we present here improves substantially over that described, in a rather sketchy fashion, in our earlier paper. That analysis used only the e^+e^- total cross section data and used the two Weinberg sum rules to determine the contribution of the a_1 . The numerical values of S which we obtain here are smaller than those of Ref. [13], mainly because τ decay data implies a larger coupling of the a_1 to the axial-vector current.

For e^+e^- annihilation into hadrons we use the data from the OLYA and CMD detectors at the Novosibirsk collider VEPP-2M [38] in the energy range 460–1400 MeV, and the Orsay detector DCI-DM2 [39] data in the energy range 1350–2400 MeV for the reactions

$$\begin{aligned} e^+e^- &\rightarrow \pi^+\pi^- \\ &\rightarrow 2\pi^+2\pi^- \\ &\rightarrow \pi^+\pi^-2\pi^0 \\ &\rightarrow 3\pi^+3\pi^- \\ &\rightarrow 2\pi^+2\pi^-2\pi^0. \end{aligned} \quad (7.12)$$

Note that the final state cannot consist of only π^0 's because of C conservation. For τ decay into hadrons we use ARGUS [40] Collaboration data, from the DESY storage ring DORIS II, for the reaction

$$\tau^- \rightarrow \nu_\tau \pi^+ 2\pi^-. \quad (7.13)$$

In both cases, we must take into account the unmeasured channels such as $e^+e^- \rightarrow \pi^+\pi^-4\pi^0$ and $\tau^- \rightarrow \nu_\tau \pi^- 2\pi^0$. This is done by assuming the simplest isospin assignments of intermediate states in the decay processes. We assess the contribution of the higher pion multiplicity channels by smoothly matching to the measured e^+e^- total cross

section at high energies. Our main interest here is to present relatively simple functions which represent the data but are amenable to scaling with N_{TF} and N_{TC} . The values of the various parameters which appear in our representation of R_V and R_A are presented in Appendix D.

The most important contribution to R_V is the $e^+e^- \rightarrow 2\pi$ channel, which is dominated by the ρ . This channel is well represented by the function [41]

$$\begin{aligned} R_\rho(s) &= \frac{1}{4} \left[1 - \frac{4m_\pi^2}{s} \right]^{3/2} \theta(s - 4m_\pi^2) \\ &\times \left[\frac{m_\rho^4}{(s - m_\rho^2)^2 + m_\rho^2 \Gamma_\rho(s)^2} \right], \end{aligned} \quad (7.14)$$

where

$$\Gamma_\rho(s) = \Gamma_\rho(m_\rho^2) \frac{m_\rho}{\sqrt{s}} \left[\frac{s - 4m_\pi^2}{m_\rho^2 - 4m_\pi^2} \right]^{3/2} \theta(s - 4m_\pi^2). \quad (7.15)$$

Note that $\Gamma_\rho(m_\rho^2)$ is given by

$$\Gamma_\rho(m_\rho^2) = \frac{g_{\rho\pi\pi}^2 m_\rho}{4\pi \cdot 12} \left[1 - \frac{4m_\pi^2}{m_\rho^2} \right]^{3/2}. \quad (7.16)$$

Therefore, (7.15) can be written as

$$\Gamma_\rho(s) = \frac{g_{\rho\pi\pi}^2 s}{48\pi m_\rho} \left[1 - \frac{4m_\pi^2}{s} \right]^{3/2} \theta(s - 4m_\pi^2), \quad (7.17)$$

which is the convenient form for rescaling. Our fit to the $e^+e^- \rightarrow \pi^+\pi^-$ data of the OLYA and CMD detectors is shown in Fig. 7(a).

To the $e^+e^- \rightarrow 4\pi$ channel data, we fit the following Breit-Wigner function:

$$R_{BW}(s) = \frac{9}{\alpha^2} \frac{m^2 \Gamma^{e^+e^-} \Gamma(s)}{(s - m^2)^2 + m^2 \Gamma(s)^2}, \quad (7.18)$$

where

$$\Gamma(s) = \Gamma(m^2) \frac{P_{LI}(s; 4\pi)}{P_{LI}(m^2; 4\pi)}. \quad (7.19)$$

$P_{LI}(s; 4\pi)$ stands for the 4-pion Lorentz-invariant phase space. The fit to the $e^+e^- \rightarrow 2\pi^+2\pi^-$ data of OLYA and DM2 is shown in Fig. 7(b).

To the $e^+e^- \rightarrow 6\pi$ channel data, we fit a function intended to represent the sum of the total cross sections to 6 and more pions:

$$R_{\text{cont}}(s) = R_{\text{asympt}} \left[\frac{\frac{\pi}{2} + \arctan \left[\frac{1}{\gamma} - \left(\gamma + \frac{1}{\gamma} \right) \frac{m^2}{s} \right]}{\frac{\pi}{2} + \arctan \left[\frac{1}{\gamma} \right]} \right] D(s). \quad (7.20)$$

This function can be interpreted as a superposition of evenly spaced Breit-Wigner resonances [42]:

$$R_{\text{cont}} \sim \sum_n \frac{9}{\alpha^2} \frac{s \Gamma_n^{e^+e^-} \Gamma_n}{(s - m_n^2)^2 + m_n^2 \Gamma_n^2} D(s) \quad (7.21)$$

with the condition

$$\Gamma_n / m_n = \text{const} \equiv \gamma, \quad \Gamma_n^{e^+e^-} \Gamma_n = \text{const}. \quad (7.22)$$

The parameter m is the mass of the lowest-lying resonance contributing to this sum. The function $D(s)$ is a damping factor for killing off the tail of $R_{\text{cont}}(s)$ in the infrared which we take to be

$$D(s) = \theta(m - \sqrt{s}) e^{-[(\sqrt{s} - m)^2 / m^2 \gamma^2]} + \theta(\sqrt{s} - m). \quad (7.23)$$

The expression (7.20) is compared to the DM2 data on $e^+e^- \rightarrow 6\pi$ in Fig. 7(c). We should note again that (7.20) represents the sum of all multipion cross sections and so tends at high energy to the asymptotic value of R_V .

Adding all these contributions together, we get the solid curve shown in Fig. 8. In the figure, our representation of $R_V(s)$ is compared to the values of $R(s)$ from OLYA, CMD [38], and the Frascati collider ADONE [43]. As we can see, our function roughly follows the contour of the $R(s)$ data. The discrepancy comes from the $I=0$ and $s\bar{s}$ channels.

To the $\tau^- \rightarrow \nu_\tau 3\pi$ channel we fit the Breit-Wigner function (7.18) except this time with

$$\Gamma(s) = \Gamma(m^2) \frac{P_{\text{LI}}(s; 3\pi)}{P_{\text{LI}}(m^2; 3\pi)}. \quad (7.24)$$

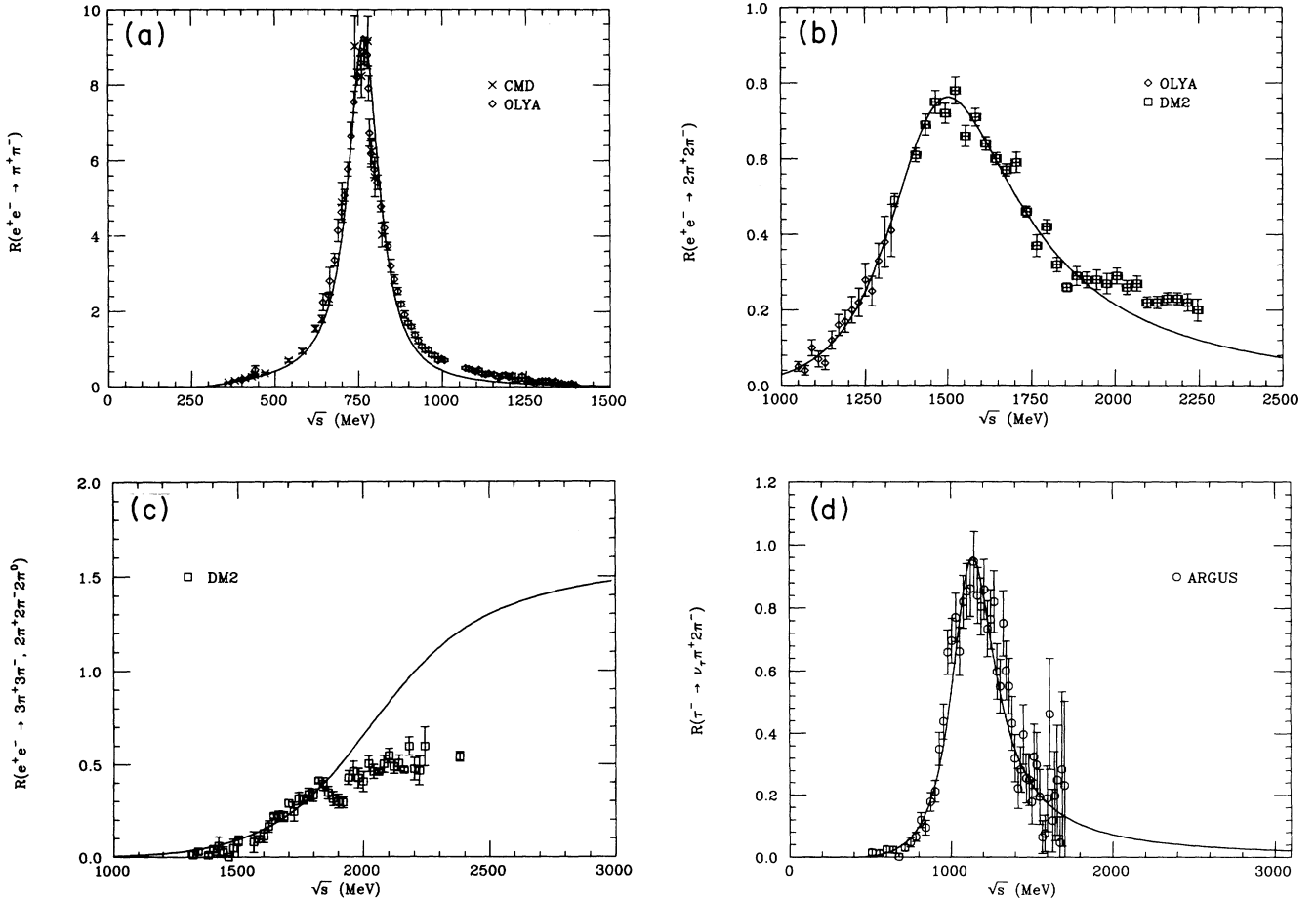


FIG. 7. Comparison of components of our parametrization of R_V and R_A to total cross-section data from the OLYA, CMD, DM2, and ARGUS experiments: (a) $e^+e^- \rightarrow \pi^+\pi^-$; (b) $e^+e^- \rightarrow 2\pi^+2\pi^-$; (c) $e^+e^- \rightarrow 6\pi$, compared to Eq. (7.20); (d) $\tau^- \rightarrow \nu_\tau \pi^+ 2\pi^-$.

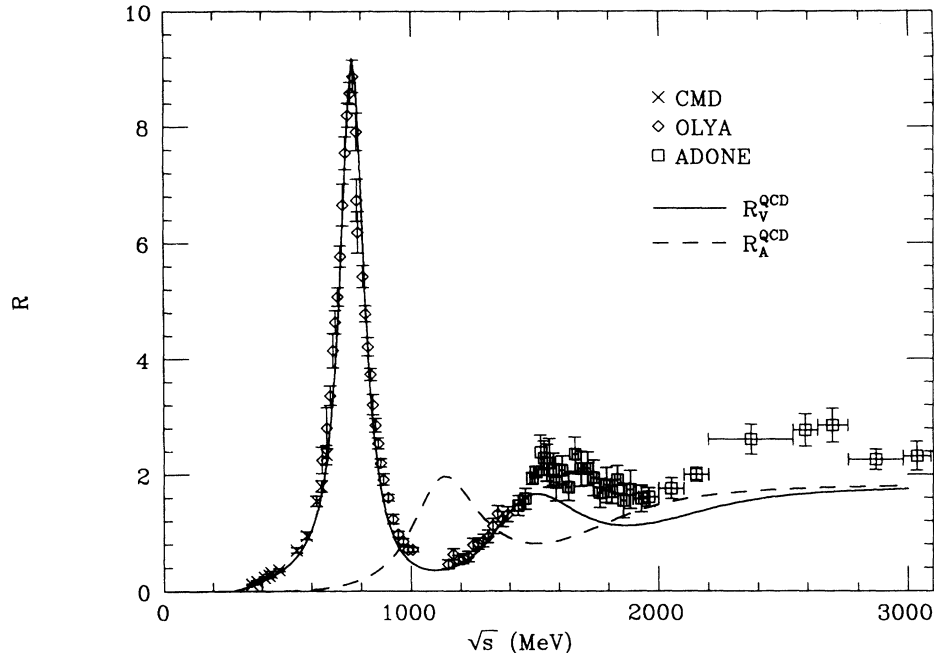


FIG. 8. Our parametrization of $R_V(s)$ (solid line) and $R_A(s)$ (broken line) for QCD. These functions are compared to the measured values of the e^+e^- total cross section $R(s)$ from OLYA, CMD, and ADONE.

$P_{\text{LI}}(s; 3\pi)$ is the 3-pion Lorentz-invariant phase space. This function is compared to the ARGUS results for $R_A(s)$ in Fig. 7(d). While we have a fit for $R_V(s)$ which goes up to roughly 3 GeV, no data are available for $R_A(s)$ above 1.8 GeV. We therefore add the function (7.20) to $R_A(s)$ in this region with its position adjusted so that the first Weinberg sum rule is satisfied. [Because the integrand of the second Weinberg sum rule has an extra power of s , the integral is dominated at higher momenta. As a result, it does not help us determine the shapes of $R_V(s)$ and $R_A(s)$ in the infrared.] The final result of this fit is the dashed line shown in Fig. 8.

Now that we have obtained a function representing the values of R_V and R_A in the familiar strong interactions, we can construct a model of R_V and R_A in a technicolor model by scaling the various fit parameters according to the predictions of the large- N expansion, just as we did for resonance parameters in (7.5). The formula (7.14) allows us to disentangle the various dependences of the 2π intermediate state on N_{TF} and N_{TC} . We represent the techni- ρ contribution to $R_V(s)$ by a sum over the various pseudo Goldstone bosons (PGB's) into which the techni- ρ can decay:

$$R_{\rho_T}(s) = \frac{1}{4} \sum_i \left[1 - \frac{4m_i^2}{s} \right]^{3/2} \theta(s - 4m_i^2) \times \left[\frac{m_{\rho_T}^4}{(s - m_{\rho_T}^2)^2 + m_{\rho_T}^2 \Gamma_{\rho_T}(s)^2} \right]. \quad (7.25)$$

In this formula,

$$\Gamma_{\rho_T}(s) = \frac{2}{N_{\text{TF}}} \frac{3}{N_{\text{TC}}} \frac{g_{\rho\pi\pi}^2}{48\pi} \frac{s}{m_{\rho_T}} \times \sum_i \left[1 - \frac{4m_i^2}{s} \right]^{3/2} \theta(s - 4m_i^2), \quad (7.26)$$

and m_i is the mass of the i th pseudoscalar technimeson. The sum runs over pairs of mesons with $I^3 = \pm 1$, including the true Goldstone bosons. The factor $(6/N_{\text{TF}}N_{\text{TC}})$ in front of the sum in (7.26) comes from the large- N rescaling of $g_{\rho\pi\pi}$ and the techni- ρ mass m_{ρ_T} is obtained from Eq. (7.5). The mass of true Goldstone boson is set to zero while the masses of the PGB's are taken from Ref. [44].

The dependence of the other pieces of R_V and R_A on N_{TF} and N_{TC} is more straightforward. The parameters of the Breit-Wigner function (7.8) and the continuum function (7.20) are rescaled according to

$$\frac{F_\pi^2}{m_{\text{TC}}^2} = \frac{N_{\text{TF}}}{2} \frac{N_{\text{TC}}}{3} \frac{f_\pi^2}{m_{\text{QCD}}^2}, \quad (7.27)$$

$$\frac{\Gamma_{\text{TC}}(m_{\text{TC}}^2)}{m_{\text{TC}}} = \frac{N_{\text{TF}}}{2} \frac{3}{N_{\text{TC}}} \frac{\Gamma_{\text{QCD}}(m_{\text{QCD}}^2)}{m_{\text{QCD}}},$$

and the entire function is multiplied by $(N_{\text{TF}}N_{\text{TC}}/6)$. The phase-space factors in (7.19) and (7.24) are calculated with massless pions and PGB's. After rescaling the vector and axial spectral functions do not necessarily converge rapidly at high energy. We thus evaluate S by cutting off the integral at a value s_+ . We choose s_+ so that the rescaled spectral functions, integrated up to this

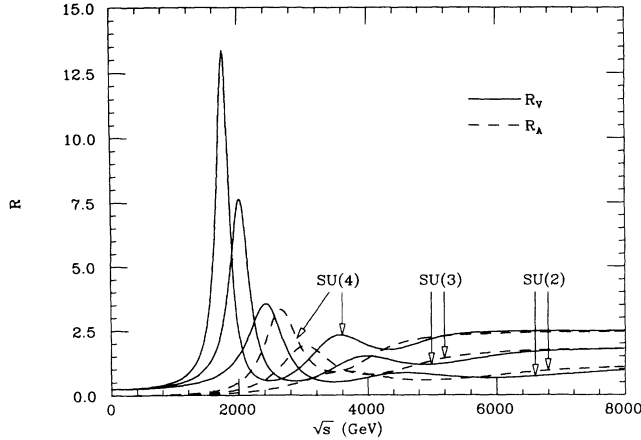


FIG. 9. $R_V(s)$ (solid line) and $R_A(s)$ (broken line) for minimal technicolor, $N_{TF}=2$, for the cases $N_{TC}=2,3,4$.

cutoff, continue to obey the first Weinberg sum rule.

We evaluate S in this scheme for two types of technicolor model. The first is the minimal model with only one doublet of technifermions ($N_{TF}=2$). The rescaled spectral functions are shown in Fig. 9 for the three cases $N_{TC}=2, 3$, and 4. We evaluate S using these spectral functions and find

$$\rho_2^0 \rightarrow \begin{cases} P_8^+ P_8^- & \text{color-octet PGB's, } m_{P_8} = 230 \text{ GeV,} \\ P_3^1 \bar{P}_3^1 + P_3^{-1} \bar{P}_3^{-1} & \text{color-triplet PGB's, } m_{P_3} = 150 \text{ GeV,} \\ P^+ P^- & \text{color-singlet PGB's, } m_P = 60 \text{ GeV,} \\ \pi_T^+ \pi_T^- & \text{technipions, } m_{\pi_T} = 0, \end{cases} \quad (7.30)$$

where we have used the notation of Ref. [45]. The masses of the color-octet and -triplet PGB's were taken from Ref. [44] while the mass of P^\pm was chosen to be larger than the experimental limit of roughly 40 GeV placed by LEP [46]. Incorporating these decays into our techni- ρ function (7.25), we obtain the spectral functions shown in Fig. 10 for the three cases $N_{TC}=2, 3$, and 4. The value of S turns out to be

$$\begin{aligned} S &\approx 0.80, & N_{TC} &= 2, \\ &\approx 1.20, & N_{TC} &= 3, \\ &\approx 1.62, & N_{TC} &= 4. \end{aligned} \quad (7.31)$$

These values should again be assigned a 25% error.

It is amusing that the results of this detailed computation are all roughly consistent with the simple formula

$$S \approx 0.3 \frac{N_{TF}}{2} \frac{N_{TC}}{3}, \quad (7.32)$$

only slightly larger than (7.6) and with the same dependence on N_{TF} and N_{TC} . In all cases, the two-pion inter-

$$\begin{aligned} S &\approx 0.22, & N_{TC} &= 2, \\ &\approx 0.32, & N_{TC} &= 3, \\ &\approx 0.45, & N_{TC} &= 4. \end{aligned} \quad (7.28)$$

For the value of $N_{TC}=3$, we estimate an error of ± 0.03 from the model dependence of the fit. The other values contain additional uncertainties due to large- N rescaling. We expect this uncertainty to be about 25%. As a check of our model of the spectrum, the value quoted for $N_{TC}=3$ should agree with the value obtained from (5.14), using the Gasser-Leutwyler [33] value of \bar{l}_5 and $m_H=380$ MeV (rescaled from 1 TeV):

$$S = \frac{1}{12\pi} \left[\bar{l}_5 + \ln \frac{m_\pi^2}{m_H^2} - \frac{1}{6} \right] = 0.309 \pm 0.034. \quad (7.29)$$

The error in (7.29) reflects the experimental uncertainty in the value of the pion charge radius and the structure term in $\pi^+ \rightarrow l^+ \nu \gamma$, from which \bar{l}_5 is obtained. The agreement of (7.29) with our determination for the case $N_{TC}=3$ is quite pleasing. To our knowledge, this is the first accurate check of the sum rule (5.12) against data from high-energy e^+e^- reactions.

The second model we considered was that with one generation of technifermions ($N_{TF}=8$). In this model, the techni- ρ decays through the following channels:

mediate state (dominated by the techni- ρ) contributes roughly 0.4 to the prefactor of (7.32); the other contributions sum to a small subtraction from this value. To our surprise, we see no sign of the quadratic dependence on

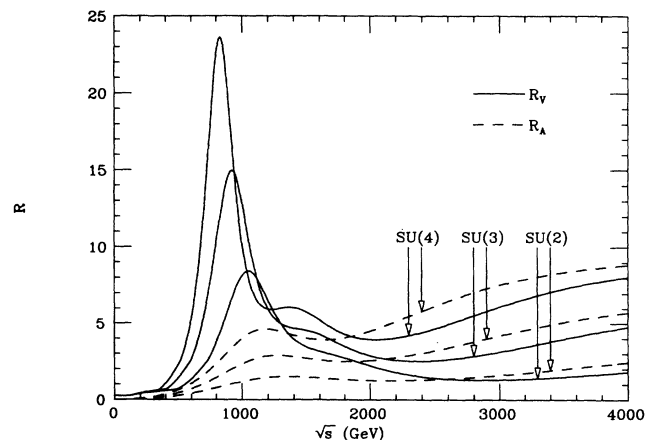


FIG. 10. $R_V(s)$ (solid line) and $R_A(s)$ (broken line) for one generation of technifermions, $N_{TF}=8$, for the cases $N_{TC}=2,3,4$.

N_{TF} indicated in (7.7) except as a redistribution of spectral weight between the techni- ρ peak and the two-pion continuum.

Using our scaled-up QCD model as a reference point, we can evaluate the effect of possible modifications of the strong-interaction spectrum due to alterations of the short-distance behavior of technicolor. One might expect two distinct effects: First, if pseudo Goldstone bosons receive large masses from extended technicolor interactions, their contribution to S is decreased. Second, if the asymptotic behavior of the hadronic vacuum polarization is altered, this can in turn alter the spectrum of resonances and thus the value of S . Let us consider these two effects in turn.

Within our model, it is straightforward to assess the effect of increasing the pseudo-Goldstone-boson masses, since these masses appear as parameters in (7.25). This formula implies that, while increasing the pseudo-Goldstone-boson masses does decrease the contribution of the mass region well below the techni- ρ , it also has the effect of making the techni- ρ a narrower and more prominent resonance. In Fig. 11, we show the effect on $R_V(s)$ of varying the pseudo-Goldstone-boson mass, assuming a common mass for all pairs of bosons into which the techni- ρ decays, and values of the other parameters appropriate to the case $N_{\text{TF}}=8$, $N_{\text{TC}}=3$. The main effect of this modification is to shift spectral weight from low mass to the techni- ρ resonance, approximately preserving the total area. The value of S decreases only slightly as the common mass m_p of the pseudo Goldstone bosons is increased. For the case $N_{\text{TF}}=8$, $N_{\text{TC}}=3$, we find a minimum of S for $m_p=400$ GeV at the value $S=1.00$, compared to $S=1.20$ in (7.31).

On the other hand, changes in the short-distance behavior may induce larger changes in S . In a recent paper, Sundrum and Hsu [47] have estimated the asymptotic behavior of the hadronic vacuum polarization in walking technicolor theories and used this to compute the effect

on S . For the case $N_{\text{TF}}=2$, $N_{\text{TC}}=3$, they find that, well above the low-lying resonances,

$$\Pi_{VV}(q^2) - \Pi_{AA}(q^2) \sim \frac{\Lambda^4}{q^2}, \quad (7.33)$$

where $\Lambda \approx 300$ MeV (F_π/f_π). To compute the change in S , Sundrum and Hsu use an exotic method of analytic continuation whose accuracy is difficult to estimate. To understand how large an effect to expect, we find it useful to apply the simple two-resonance model discussed at the beginning of this section, using (7.33) as a replacement for the second Weinberg sum rule. We find that the formula for S given in (7.4) is corrected by a term

$$\Delta S = -\frac{4\pi\Lambda^4}{m_{\rho_T}^2 m_{a_{1T}}^2} \approx -0.1. \quad (7.34)$$

This is a substantial decrease. However, this calculation represents a worst case, the assumption that, while the asymptotic behavior of the vacuum-polarization changes, this function is still dominated by the two lowest-lying resonances. This is quite unlikely, especially since the second Weinberg sum rule is rigorously valid (although very slowly convergent) in walking technicolor theories. But if we model the change in the vector spectral function as a change in the contribution of the second, rather than the lowest, resonance, the correction (7.34) decreases to 0.03 and is within the noise of our large- N rescaling.

Thus, we have some confidence that the simple formula (7.32) gives a reasonable value of S not only in the simple technicolor models based on scaled-up strong interactions but also in modified, more realistic models of technicolor dynamics. In all cases, the contribution to S in technicolor models is much larger than the value we would naively obtain from (4.2),

$$S \approx \frac{1}{6\pi} \left[\frac{N_{\text{TF}} N_{\text{TC}}}{2} \right]. \quad (7.35)$$

The factor of 2 enhancement from (7.35) to (7.32) is a low-energy signature of the presence of new strong interactions at the TeV energy scale.

VIII. ESTIMATION OF T

Up to this point in our consideration of technicolor theories, we have concentrated on the effects of technicolor interactions on S while ignoring their effects on T . However, there are good reasons to expect that T is also substantially modified by technicolor interactions. Contributions to T arise from interactions which break custodial SU(2) symmetry. In any realistic technicolor model, such breaking must be present in order that the two quarks or leptons belonging to the same SU(2) multiplet receive different masses from the dynamical symmetry breaking.

However, such isospin-breaking effects are extremely difficult to estimate. For a systematic calculation using the λ -expansion technique discussed in Sec. VI, we must include the next-to-leading-order diagrams in λ to get a result comparable to the standard-model calculations.

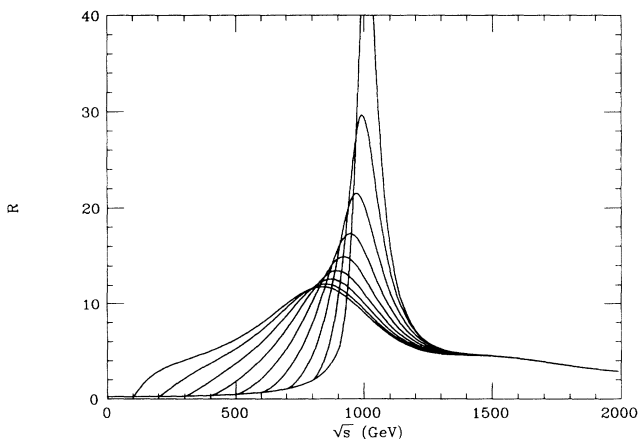


FIG. 11. The shape of the techni- ρ resonance as a function of the PGB mass for the case $N_{\text{TF}}=8$, $N_{\text{TC}}=3$. The 15 pairs of PGB's, into which the techni- ρ decays, are given a common mass m_p which is varied from 50 to 450 GeV at 50 GeV intervals.

This is because the analog of the standard-model diagram shown in Fig. 12(a) is given by the diagram shown in Fig. 12(b). Therefore, in order to calculate T , we need not only the two current correlator (vacuum polarization) but also the three and four current correlators. Whereas the two current correlator can be treated by writing a dispersive integral, it is much more difficult to represent and evaluate the higher-point functions in a general strong-interaction theory. In addition, even the leading-order contribution in λ is uncertain, because it involves the difference of charged and neutral spectral functions, which arises from perturbations of the basic strong-interaction dynamics.

In addition, the major source of isospin violation in technicolor models is the extended technicolor interaction. The form of this interaction is usually the most model-dependent part of a realistic theory of technicolor. A further complication comes from the fact that the isospin mass splitting of the (t, b) doublet is extremely large. In constructing a model of extended technicolor, it is usually a difficult problem to allow enough isospin violation to generate a large top-quark mass while restraining this isospin violation from generating a large correction to the ρ parameter or, in our notation, to T .

In the literature, two methods have been proposed to solve this problem. In Refs. [7,48], it was proposed that extended technicolor could generate a large top-quark mass by enhancing the effect of hypercharge interactions, which naturally create a larger condensate for the charge $+\frac{2}{3}$ member of a doublet of techniquarks. The authors of Ref. [7] estimated the effect of this mechanism on T by evaluating vacuum-polarization loops of noninteracting technifermions with running masses $\Sigma_U(k^2)$ and $\Sigma_D(k^2)$:

$$T = \frac{N_{\text{TC}}}{16\pi s^2 c^2 m_Z^2} \times \int_0^\infty dk^2 k^4 \left[\frac{1}{k^2 + \Sigma_U^2(k^2)} - \frac{1}{k^2 + \Sigma_D^2(k^2)} \right]^2. \quad (8.1)$$

The momentum dependence of the Σ 's were obtained by solving the gap equation. The approximation which leads to (8.1) is valid at momentum scales much higher than the technicolor scale where technicolor interactions are asymptotically free. However, the integral is dominated by the contribution from the technicolor scale which makes this estimate highly unreliable.

If we neglect the momentum dependence of the Σ 's and crudely assume $\Sigma_U - \Sigma_D = m_t$, then (8.1) is reduced to (4.2) and we find

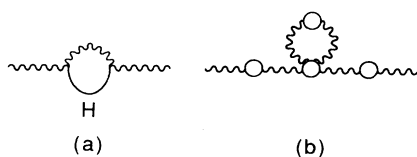


FIG. 12. Comparison of leading diagrams contributing to T in the standard loop expansion and the λ expansion.

$$T = \left[\frac{3m_t^2}{16\pi s^2 c^2 m_Z^2} \right] \left[\frac{4N_{\text{TC}}}{9} \right]. \quad (8.2)$$

The factor in the parentheses is the standard t -quark contribution. Note that if the technifermion doublet carries color, (8.2) must be multiplied by a factor of 3. The values of T for technicolor shown in Fig. 1 of Ref. [13] were obtained from (8.2). This simple approximation is not a bad representation of the more sophisticated numerical evaluate of (8.1) given in Ref. [7]. Even with that more careful evaluation, the contribution of (8.1) to T is expected to be dangerously large if $m_t > 100$ GeV.

A second method for obtaining a large m_t , explored by King and Mannan [49] and by Einhorn and Nash [50], places the isospin asymmetry in the spectrum of extended technicolor gauge bosons. The lightest of these bosons generates the top-quark mass. These authors have obtained specific models with in which the contribution to T is only a few tenths. The final result, though, is sensitive to the detailed structure of the technifermion condensate as well as to the explicit coupling of extended technicolor.

These two estimates of the contribution to T share the feature that they are highly uncertain, both because they are based on arbitrary and unsystematic reductions of the full set of contributions to T and because they use crude approximations to strong-interaction dynamics. It is unlikely that anyone would claim that technicolor models are ruled out if the true value of T turns out to be much smaller than (8.2); the problem would simply be returned to the theorists for a better calculation or a better model. We consider it an important problem to devise a more rigorous representation for T , which might be useful in computing T more accurately in any given model for extended technicolor. But even if T could be computed accurately in a given model, the model dependence of this quantity limits its usefulness as a means of confirming or excluding the idea of technicolor.

IX. EXPERIMENTAL LIMITS ON S AND T

In this section, we will discuss the determination of S and T using the values of weak-interaction observables. In particular, we will be interested in what constraints we can put on S independently of T . We will see that, even if T cannot be reliably estimated in technicolor models, the present constraints on S are sufficiently strong to exclude technicolor models with a full generation of technifermions.

Since the appearance of Ref. [13], a number of authors have presented fits of weak-interaction data in terms of S and T or related parameters [14–18]. Because of the dramatic improvement in the measured values of the Z^0 parameters and asymmetries from LEP, the constraints on S and T are now considerably stronger than those which could be obtained in the summer of 1990. The analysis we will present in this section is quite similar to the recent fits of Bhattacharyya, Banerjee, and Roy [18] and Altarelli, Barbieri, and Jadach [16], and our conclusions agree substantially with those of these authors. Given the progress of weak-interaction experimentation,

it will also probably very soon be obsolete. But we feel it is a valuable part of our general review of the (S, T) parametrization to explain the physics behind the experimental determination of S and T .

In our formalism, each observable x depends linearly on S and T . Let us write the relation for a general observable x as

$$x(S, T) = x_{\text{SM}}(m_t, m_H) + a_x S + b_x T, \quad (9.1)$$

where $x_{\text{SM}}(m_t, m_H)$ is the standard-model prediction, computed at the reference values of m_t , and m_H . In Appendix B, we list these formulas for various observables with $m_t = 150$ GeV and $m_H = 1$ TeV. According to (9.1), a precise experimental determination of x will restrict S and T to lie on a line in the S - T plane. By intersecting the lines corresponding to different observables, we can determine S and T and also, eventually, test the consistency of the restriction to a two-parameter space. In practice, experimental measurements have associated errors, so that the lines become bands in the S - T plane, and we must give a statistical criterion for their overlap.

The key to a determination of S and T is the fact that different observables give lines of different slope in the S - T plane. By inspecting the table in Appendix B, we can see that the various weak-interaction observables are to be separated by their S and T dependence into three general classes. In the first class are observables with relatively weak dependence on S compared to T . This class includes parameters R_ν and g_L^2 which measure the charged- to neutral-current ratio in neutrino scattering, the various partial widths of the Z^0 , and, with only a slightly stronger S dependence, the mass of the W . In other words, this class includes all of the weak-interaction observables which were known with high precision prior to the summer of 1990. The second class includes the Z^0 asymmetries, quantities which depend on S and T through $s_*^2(m_Z^2)$. The relative sensitivity of these

quantities to S is made clear, for example, by comparing the first two lines of (3.13).

Finally, there is a third class of measurements which are almost insensitive to T and so measure S directly. Marciano and Rosner [14] and Sandars [55] recognized that the strength of atomic parity violation has this property. To see why, take the matrix element of the low-energy effective Lagrangian (2.24) and consider the piece which involves the axial-vector current of the electron times and coherent vector current matrix element in the atomic nucleus. This gives the following expression for the weak charge which determines the magnitude of atomic parity violation:

$$Q_W = -\rho_*(0) \{ N - [1 - 4s_*^2(0)]Z \}, \quad (9.2)$$

where N, Z are the number of neutrons and protons in the nucleus. Expression (9.2) depends on T through both of the starred functions. The two T -dependent terms are

$$-(\alpha T)[N - (1 - 4s^2)Z] + \frac{4\alpha s^2 c^2}{c^2 - s^2} ZT. \quad (9.3)$$

For the particular neutron content of cesium, $N/Z = 1.41$, the second term of (9.3) cancels 95% of the first term. A similar cancellation would hold for most elements in the lower half of the periodic table. Krauss [56] has pointed out that the same cancellation occurs in the cross section for coherent neutral-current neutrino scattering, which will eventually be observed by bolometric detectors. Unfortunately, the cancellation does not occur in the isotope effect in atomic parity violation, the coefficient of N in (9.2), which has been proposed as an observable with a lower theoretical systematic error than Q_W [57]. This latter observable belongs to the first class and so must compete with Γ_Z and R_ν in its significance for weak-interaction theory.

In Figs. 13 and 14, we show the present constraints on

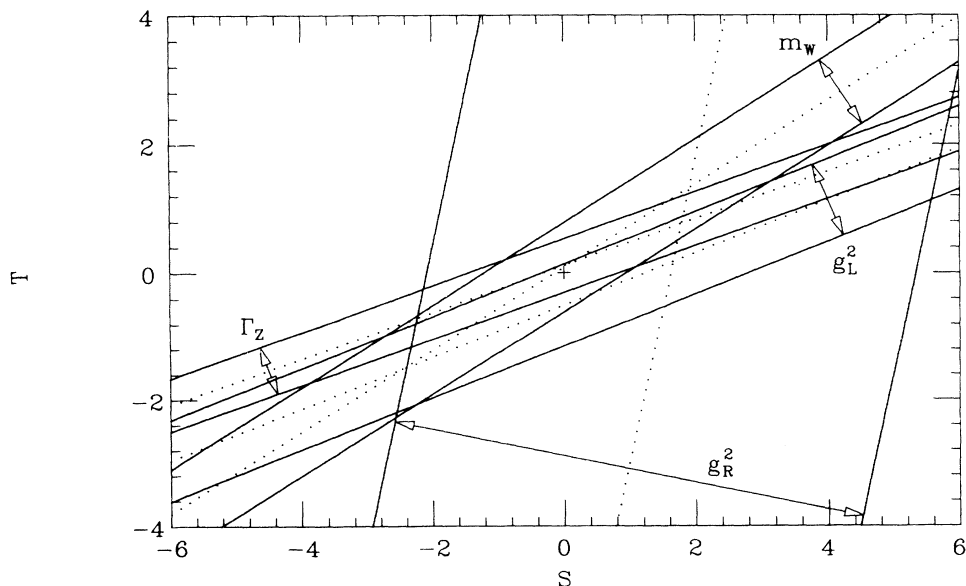


FIG. 13. Bands in the S - T plane allowed, within the 1σ errors, by the first four measurements listed in Table I. These observables belong to the first class discussed in the text.

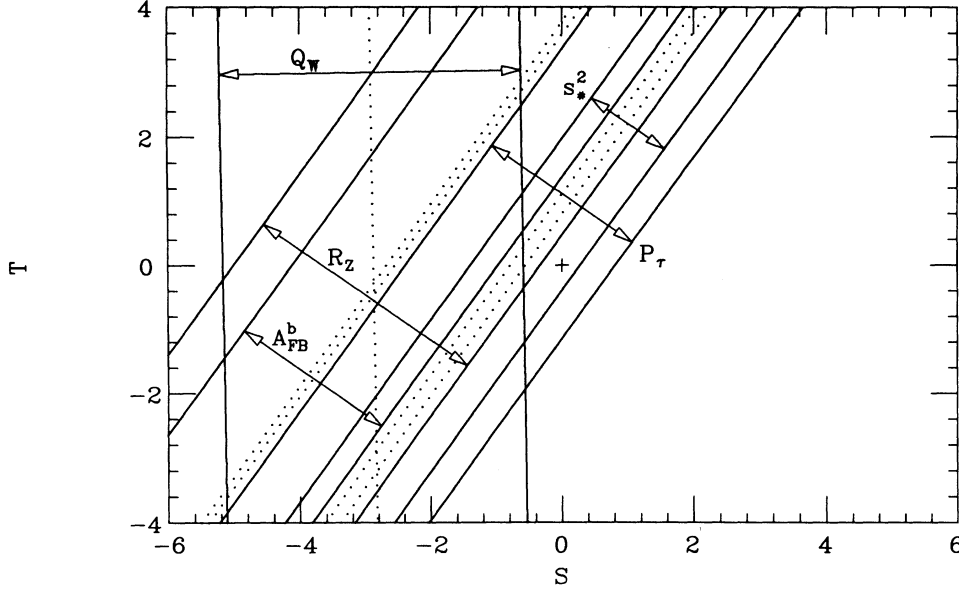


FIG. 14. Bands in the S - T plane allowed, within 1σ errors, by the last five measurements listed in Table I. These observables belong to the second and third classes discussed in the text.

S and T from the measurement of the set of weak-interaction parameters listed in Table I. The experimental values are plotted as bands in the S - T plane whose boundaries correspond to the 1σ errors. Figure 13 shows the best-measured variables of the first class (plus the value of g_R^2 , which is obtained from the difference of R_ν and $R_{\bar{\nu}}$). Figure 14 shows the quite different constraint which comes from the second and third classes of observables.

Just by inspection we can see that the overlap of the bands is greatest in the third quadrant of the S - T plane. To describe this overlap more quantitatively, we construct the likelihood function of S and T , given by [58]

$$L(x_{\text{expt}}; S, T) = N \exp \left[- \sum_x \frac{1}{2} \left(\frac{x_{\text{expt}} - x(S, T)}{\sigma_x} \right)^2 \right], \quad (9.4)$$

where the normalization factor N is such that

$$\int dS dT L(x_{\text{expt}}; S, T) = 1. \quad (9.5)$$

The point which maximizes $L(x_{\text{expt}}; S, T)$ is found to be

$$(S, T) = (-1.52, -0.69). \quad (9.6)$$

Figures 15 and 16 show this point and the 68% and 90% confidence level contours around it. In order to obtain the limits on S independent of T , we integrate $L(x_{\text{expt}}; S, T)$ over T to obtain a likelihood function of only S :

$$L(x_{\text{expt}}; S) = \int_{-\infty}^{\infty} dT L(x_{\text{expt}}; S, T) \quad (9.7)$$

and interpret the quantity

$$p(S < \bar{S}) = \int_{-\infty}^{\bar{S}} dS L(x_{\text{expt}}; S) \quad (9.8)$$

as the probability that $S < \bar{S}$. The 90% and the 95% one-sided upper confidence limits obtained from (9.8) are shown with the larger notches on the lower part of Fig. 15. This determination corresponds to $S = -1.52 \pm 0.84$.

Let us emphasize that these limits on S and T refer specifically to their definition as deviations from the standard model with the reference values $m_t = 150$ GeV,

TABLE I. Measurements entering our determination of S and T . The value of $s_*^2(m_Z^2)$ listed is that determined from A_{FB}^b . The standard-model predictions are given for the reference conditions $m_t = 150$ GeV, $m_H = 1$ TeV.

Observable	Measured value	Reference	Standard model
m_W/m_Z	0.8791 ± 0.0034	[51]	0.8787
Γ_Z [GeV]	2.487 ± 0.009	[23]	2.484
g_L^2	0.2977 ± 0.0042	[52]	0.3001
g_R^2	0.0317 ± 0.0034	[52]	0.0302
R_Z	20.94 ± 0.12	[23]	20.78
$s_*^2(m_Z^2)$	0.2317 ± 0.0030	[23]	0.2337
A_{FB}^b	0.135 ± 0.031	[23]	0.0848
P_τ	-0.152 ± 0.045	[53]	-0.1297
$Q_W(^{133}\text{Cs})$	-71.04 ± 1.81	[54]	-73.31

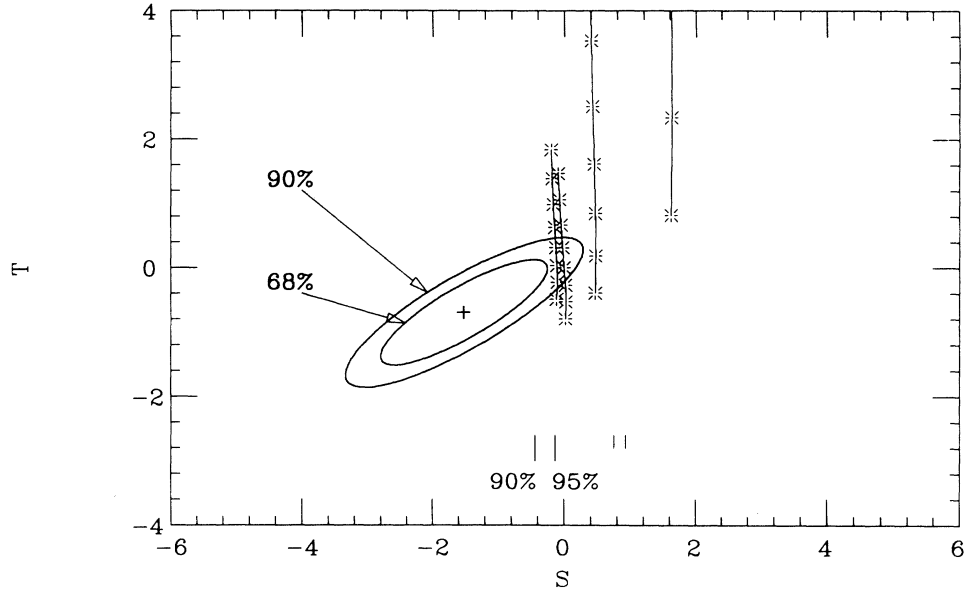


FIG. 15. Contours of the likelihood function of S and T corresponding to 68% and 90% probability, computed from the measurements listed in Table I. The long notches at the bottom of the figure correspond to the 90% and 95% confidence upper limits on S in an unbiased analysis. The shorter notches show the locations of these limits if one imposes *a priori* that $S > 0$.

$m_H = 1$ TeV. For different values of m_t and m_H , the position of the likelihood contours on the S - T plane will be different. However, the shapes and sizes of these contours would be the same. This gives a convenient way to plot the influence of the reference m_t and m_H on the S - T analysis: We simply hold the position of the likelihood

contours fixed and plot the relative position of the origin with respect to these contours. As we vary m_t , this relative position then sweeps out a contour in the S - T plane which roughly follows the displacements (4.4) but gives a more accurate accounting for small values of m_t . In Figs. 15 and 16, we have plotted the contours corre-

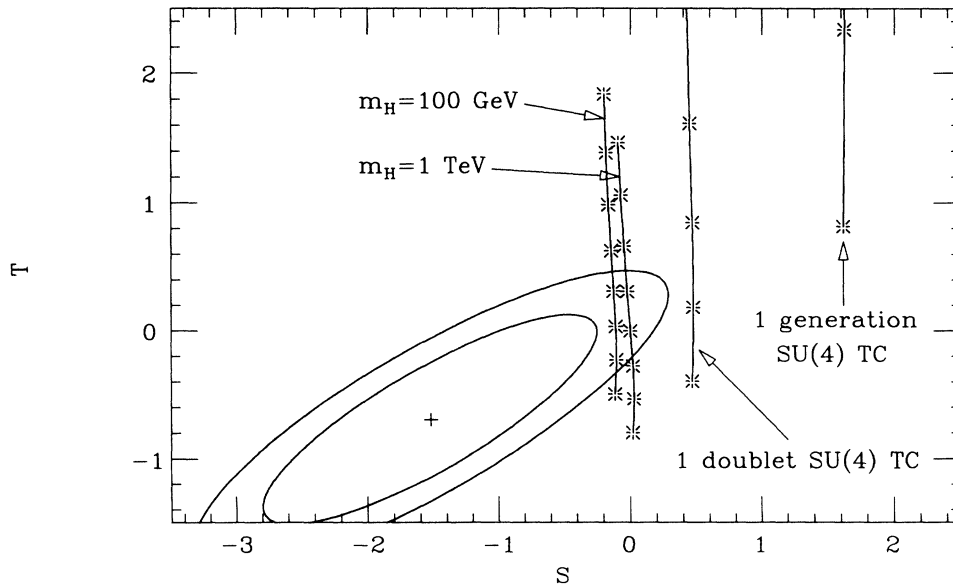


FIG. 16. Enlarged version of Fig. 15, showing the comparison of the region preferred by the fit with the predictions of the minimal standard model and two technicolor models. The values of S and T for the minimal standard model are computed as described in the text, for Higgs-boson masses for 100 GeV and 1 TeV, as a function of the top-quark mass. The stars denote values of m_t from 75 to 250 GeV in 25 GeV steps. The values of S in technicolor models are the values for $N_{TC} = 4$ from Sec. VII. The values of T due to technicolor are computed from (8.2), as an indication of the possible size of this effect. Again, the stars denote values of m_t increasing from 75 GeV in steps of 25 GeV.

sponding to Higgs-boson masses of 1 TeV and 100 GeV. We find this plot a useful way to view the precision weak-interaction data even in reference to the minimal standard model. For example, the subtle preference of the data for lower values of m_H , noted by many authors, is apparent in these figures.

We have also plotted in the two figures our estimates of S and T for technicolor models with one doublet and one generation of technifermions. The estimate for S is that given in (7.28) and (7.31), and the estimates for T were obtained from (8.2). It seems that the data does not particularly favor either choice and seems quite inconsistent with the 1 generation case.

In fact, it is noteworthy that, whereas the standard model gives small values of S and the corrections due to technicolor are positive, the experimental results favor a sizable negative value of S . This makes it difficult to state the precise constraint on technicolor models that the data provides. A conservative criterion is the following: let us assume *a priori* that the value of S is positive. Then the *a posteriori* probability that $S < \bar{S}$ is given by

$$p(S < \bar{S}) = \frac{\int_0^{\bar{S}} dS L(x_{\text{expt}}; S)}{\int_0^{\infty} dS L(x_{\text{expt}}; S)}. \quad (9.9)$$

This criterion gives slightly weaker 90% and 95% one-sided upper confidence limits, which are shown with the unmarked smaller notches on Fig. 15. In particular, we conclude that technicolor models must satisfy the constraint

$$S < 0.93 \quad (95\% \text{ C.L.}). \quad (9.10)$$

We emphasize that this is a new constraint for technicolor models, independent of previous constraints from flavor-changing neutral currents or the ρ parameter, and one which is much less dependent on the details of technicolor and extended technicolor model building. We have argued in Sec. VII that this bound excludes technicolor models with a full generation of technifermions except in special limiting circumstances.

Given the rate of progress in weak-interaction experimentation, we feel confident that the results quoted in Table I, and thus the bounds we have quoted on S and T , will soon be obsolete. We encourage experimenters, especially experiments involving the Z^0 parameters and deep-inelastic neutrino scattering which measure several observables, to present limits on S and T from their own experimental data as a complement to their more conventional fits to $\sin^2\theta_W, m_t, m_H$. We are pleased that the ALEPH Collaboration experiment has already published a determination of S based only on their own data and taking into account the correlations and asymmetric errors of data points in a proper way [59]. Converted to our conventions, their result is $S = -1.9 \pm 1.1$; this compares favorably with the end result of our global analysis. Though the ALEPH paper reaches S through the determination of partial widths and asymmetries, it is also straightforward, and may eventually be more effective, to fit the measured differential cross sections directly to functions of S and T [60].

To give an idea of the accuracy which should be

achievable, we have evaluated the constraint on S which would follow, later in this decade, from the following set of precision measurements: m_W to 100 meV; Γ_Z to 6 MeV (the systematic error in the theoretical prediction due to the uncertainty in α_s); A_{FB}^b to 0.005; and A_{LR} to 0.01. This set of measurements would determine S to ± 0.35 . If A_{LR} could be measured to 0.003, S will be known to ± 0.23 . This is approximately equal to $4/6\pi$, the shift of S due to one heavy generation.

There remains the question of whether, if the negative central value of S is confirmed, there is a model which can account for this. We do not know a simple model which gives such a large negative value of S . Recent works by Bertolini and Sirlin [61], and Gates and Terning [62] suggest that one may be able to construct a model which predicts negative values for both S and T by including Majorana particles. Dugan and Randall [63] and Georgi [64] have given other examples of weak quantum number assignments which lead to a negative value of S . Whether such an approach leads to a realistic theory which is compatible with the limits on S and T remains to be seen.

X. CONCLUSIONS

In this paper, we reviewed the general analysis of the oblique electroweak corrections to precision measurements. We started by reviewing the formalism of Kennedy and Lynn which summarized the effect of oblique corrections into the starred functions. A momentum expansion of the vacuum-polarization amplitudes let us reduce the starred functions to just three parameters S , T , and U .

The use of dispersion relations let us estimate S for strongly interacting theories in which perturbation theory cannot be used. For QCD-like technicolor, we found S to be positive and roughly proportional to the number of technifermion doublets.

Analysis of the precision electroweak measurements puts a limit on S and T . The experimentally favored value of S turns out to be negative which rules out QCD-like technicolor theories with a large technisector.

Constructing a model which predicts negative values for S and T , and finding a reliable method for estimating T from theory remain as open problems.

ACKNOWLEDGMENTS

We are grateful to A. Blondel, J. Bjorken, M. Golden, T. Hansl-Kozanecka, D. Kennedy, K. Lane, P. Langacker, B. Lynn, L. Randall, J. Rosner, R. Sundrum, M. Swartz, K. Takeuchi, and T. Troung for helpful discussions, and to J. Lauer for a critical reading of this manuscript. A portion of this work was presented at the 1991 Aspen Winter Conference, January 6–12, 1991, and at the ITP Topical Conference on Precise Electroweak measurements, February 21–23, 1991, Santa Barbara. This work was supported by the Department of Energy, Contract No. DE-AC03-76SF00515.

APPENDIX A

In this appendix, we tabulate the dependence of various observables on oblique radiative corrections, by ex-

pressing their dependence on the starred functions. These formulas can be used to derive the (S, T) dependences of observables listed in Appendix B. One should note that certain observables, in particular $\Gamma_{b\bar{b}}$ and A_{FB}^b , can receive sizable nonstandard corrections from vertex diagrams in specific models. On the other hand, these expressions are not adequate for deriving the standard-model predictions for these observables, since there are nontrivial parts of vertex and box diagrams can be important. QCD corrections are included in N_{quark} and k_A .

Z^0 widths:

$$\begin{aligned}\Gamma_Z &= Z_{Z^*} \frac{\alpha_* m_Z}{6s_*^2 c_*^2} \sum_f (I_{3f} - s_*^2 Q_f)^2 \Big|_{q^2=m_Z^2} \\ &= 3\Gamma_{\nu\bar{\nu}} + 3\Gamma_{l+l^-} + \Gamma_{\text{had}} , \\ \Gamma_{\nu\bar{\nu}} &= Z_{Z^*} \frac{\alpha_* m_Z}{24s_*^2 c_*^2} \Big|_{q^2=m_Z^2} , \\ \Gamma_{l+l^-} &= Z_{Z^*} \frac{\alpha_* m_Z}{6s_*^2 c_*^2} \left[\left(-\frac{1}{2} + s_*^2\right)^2 + (s_*^2)^2 \right] \Big|_{q^2=m_Z^2} , \\ \Gamma_{u\bar{u}} &= \Gamma_{c\bar{c}} \\ &= Z_{Z^*} \frac{\alpha_* m_Z}{6s_*^2 c_*^2} \left[\left(\frac{1}{2} - \frac{2}{3}s_*^2\right)^2 + \left(-\frac{2}{3}s_*^2\right)^2 \right] N_{\text{quark}} \Big|_{q^2=m_Z^2} , \\ \Gamma_{d\bar{d}} &= \Gamma_{s\bar{s}} = \Gamma_{b\bar{b}} \\ &= Z_{Z^*} \frac{\alpha_* m_Z}{6s_*^2 c_*^2} \left[\left(-\frac{1}{2} + \frac{1}{3}s_*^2\right)^2 + \left(\frac{1}{3}s_*^2\right)^2 \right] N_{\text{quark}} \Big|_{q^2=m_Z^2} , \\ \Gamma_{\text{had}} &= 2\Gamma_{u\bar{u}} + 3\Gamma_{d\bar{d}} .\end{aligned}$$

Asymmetries at the Z^0 pole:

$$\begin{aligned}A_{LR} &= \left[\frac{(g_{L^*}^e)^2 - (g_{R^*}^e)^2}{(g_{L^*}^e)^2 + (g_{R^*}^e)^2} \right] \\ &= \frac{[-\frac{1}{2} + s_*^2(q^2)] - [s_*^2(q^2)]^2}{[-\frac{1}{2} + s_*^2(q^2)]^2 + [s_*^2(q^2)]^2} \\ &= \frac{2[1 - 4s_*^2(q^2)]}{1 + [1 - 4s_*^2(q^2)]^2} , \\ A_{\text{FB}}^b &= \frac{3}{4} A_{LR} \left[\frac{(g_{L^*}^b)^2 - (g_{R^*}^b)^2}{(g_{L^*}^b)^2 + (g_{R^*}^b)^2} \right] \left[1 - k_A \frac{\alpha_s}{\pi} \right] \\ &= \frac{3}{4} A_{LR} \frac{[-\frac{1}{2} + \frac{1}{3}s_*^2(q^2)]^2 - [\frac{1}{3}s_*^2(q^2)]^2}{[-\frac{1}{2} + \frac{1}{3}s_*^2(q^2)]^2 + [\frac{1}{3}s_*^2(q^2)]^2} \\ &\quad \times \left[1 - k_A \frac{\alpha_s}{\pi} \right] , \\ A_{\text{FB}}^l &= \frac{3}{4} (A_{LR})^2 , \\ P_\tau &= - \left[\frac{(g_{L^*}^l)^2 - (g_{R^*}^l)^2}{(g_{L^*}^l)^2 + (g_{R^*}^l)^2} \right] = -A_{LR} .\end{aligned}$$

Deep-inelastic neutrino scattering:

$$\begin{aligned}g_L^2 &= \rho_*(0)^2 [(g_{L^*}^u)^2 + (g_{L^*}^d)^2] \\ &= \rho_*(0)^2 \left[\frac{1}{2} - s_*^2(0) + \frac{5}{9}s_*^4(0) \right] , \\ g_R^2 &= \rho_*(0)^2 [(g_{R^*}^u)^2 + (g_{R^*}^d)^2] \\ &= \rho_*(0)^2 \left[\frac{5}{9}s_*^4(0) \right] , \\ R_\nu &= g_L^2 + r g_R^2 \\ &= \rho_*(0)^2 \left[\frac{1}{2} - s_*^2(0) + \frac{5}{9}(1+r)s_*^4(0) \right] , \\ R_{\bar{\nu}} &= g_L^2 + \frac{g_R^2}{r} \\ &= \rho_*(0)^2 \left[\frac{1}{2} - s_*^2(0) + \frac{5}{9} \left[1 + \frac{1}{r} \right] s_*^4(0) \right] .\end{aligned}$$

Atomic parity violation:

$$\begin{aligned}C_{1u} &= 2\rho_*(0)(g_{L^*}^e - g_{R^*}^e)(g_{L^*}^u + g_{R^*}^u) \\ &= \rho_*(0) \left[-\frac{1}{2} + \frac{4}{3}s_*^2(0) \right] , \\ C_{1d} &= 2\rho_*(0)(g_{L^*}^e - g_{R^*}^e)(g_{L^*}^d + g_{R^*}^d) \\ &= \rho_*(0) \left[\frac{1}{2} - \frac{2}{3}s_*^2(0) \right] , \\ Q_W(Z, N) &= -2[(2Z+N)C_{1u} + (Z+2N)C_{1d}] \\ &= -\rho_*(0) \{ N - [1 - 4s_*^2(0)]Z \} .\end{aligned}$$

APPENDIX B

The following numbers are evaluated with $m_t = 150$ GeV, $m_H = 1000$ GeV, $e^2 = 4\pi\alpha_{*,0}(m_Z^2) = 4\pi/129$, $s^2 = \sin^2\theta_0 = 0.23$, and $\alpha_s = 0.12$. The constant terms on the right-hand sides are the standard-model predictions including oblique and direct corrections, and QED and QCD corrections. They are dependent on the values of m_t and m_H while the coefficients of S , T , and U are not. For example, the standard-model predictions for $\Gamma_{d\bar{d}}$ and $\Gamma_{b\bar{b}}$ differ due to the fact that $\Gamma_{b\bar{b}}$ receives an m_t -dependent correction from the vertex diagrams containing the t quark. However, the coefficients for S and T are the same because the oblique corrections are common. To evaluate R_ν and $R_{\bar{\nu}}$, we have used the CERN-Dortmund-Heidelberg-Saclay (CDHS) [65] Collaboration values of r . Other experiments should use their own measured values of r together with the formulae for g_L^2, g_R^2 below:

$$\begin{aligned}\frac{m_W}{m_Z} &= 0.8787 - (3.15 \times 10^{-3})S + (4.86 \times 10^{-3})T \\ &\quad + (3.70 \times 10^{-3})U , \\ \Gamma_Z &= 2.484 - (9.58 \times 10^{-3})S + (2.615 \times 10^{-2})T \text{ (GeV)} , \\ \Gamma_{l+l^-} &= 0.0835 - (1.91 \times 10^{-4})S + (7.83 \times 10^{-4})T \\ &\quad \text{(GeV)} , \\ \Gamma_{u\bar{u}} &= 0.2962 - (1.92 \times 10^{-3})S + (3.67 \times 10^{-3})T \text{ (GeV)} ,\end{aligned}$$

$$\begin{aligned}\Gamma_{d\bar{d}} &= 0.3823 - (1.72 \times 10^{-3})S + (4.20 \times 10^{-3})T \text{ (GeV)}, \\ \Gamma_{b\bar{b}} &= 0.3779 - (1.72 \times 10^{-3})S + (4.20 \times 10^{-3})T \text{ (GeV)}, \\ \Gamma_{\text{had}} &= 1.7348 - (9.00 \times 10^{-3})S + (1.993 \times 10^{-2})T \\ &\text{(GeV)},\end{aligned}$$

$$\begin{aligned}R_Z &= \Gamma_{\text{had}}/\Gamma_{l+l^-} \\ &= 20.78 - (5.99 \times 10^{-2})S + (4.24 \times 10^{-2})T, \\ s_*^2(m_Z^2) &= 0.2337 + (3.59 \times 10^{-3})S - (2.54 \times 10^{-3})T, \\ A_{LR} &= -P_\tau = 0.1297 - (2.82 \times 10^{-2})S + (2.00 \times 10^{-2})T, \\ A_{\text{FB}}^b &= 0.0848 - (1.97 \times 10^{-2})S + (1.40 \times 10^{-2})T, \\ A_{\text{FB}}^l &= 0.0126 - (6.72 \times 10^{-3})S + (4.76 \times 10^{-3})T, \\ g_L^2 &= 0.3001 - (2.67 \times 10^{-3})S + (6.53 \times 10^{-3})T, \\ g_R^2 &= 0.0302 + (9.17 \times 10^{-4})S - (1.94 \times 10^{-4})T, \\ R_\nu &= 0.3126 - (2.32 \times 10^{-2})S + (6.46 \times 10^{-2})T \\ &\quad (r=0.383), \\ R_{\bar{\nu}} &= 0.3824 - (2.77 \times 10^{-3})S + (6.03 \times 10^{-3})T \\ &\quad (r=0.371), \\ Q_W(^{133}\text{Cs}) &= -73.31 - 0.790S - 0.011T,\end{aligned}$$

APPENDIX C

In this appendix, we clarify the relation of the parameters of oblique corrections defined in Sec. III to those of other authors.

First of all, we would like to clarify precisely how our formalism is a specialization of the formalism of Kennedy and Lynn [12]. As a part of their analysis, Kennedy and Lynn defined a running Fermi constant $G_{F*}(q^2)$ and a running ρ parameter $\rho_*(q^2)$ as

$$\begin{aligned}\frac{1}{4\sqrt{2}G_{F*}(q^2)} &= \frac{v^2}{4} + [\Pi_{11}(q^2) - \Pi_{3Q}(q^2)], \\ \frac{1}{\rho_*(q^2)} &= 1 - 4\sqrt{2}G_{F*}(q^2)[\Pi_{11}(q^2) - \Pi_{33}(q^2)].\end{aligned}\quad (\text{C1})$$

These functions enable us to write

$$\begin{aligned}\frac{Z_{Z*}}{q^2 - M_{Z*}^2} &= \frac{1}{q^2 - \frac{e_*^2}{s_*^2 c_*^2} \frac{1}{4\sqrt{2}G_{F*}\rho_*}}, \\ \frac{Z_{W*}}{q^2 - M_{W*}^2} &= \frac{1}{q^2 - \frac{e_*^2}{s_*^2} \frac{1}{4\sqrt{2}G_{F*}}}\end{aligned}$$

Therefore, in the original version of the Kennedy-Lynn formalism, the effects of oblique corrections were summarized in the four starred functions: $e_*^2(q^2)$, $s_*^2(q^2)$, $G_{F*}(q^2)$, and $\rho_*(q^2)$.

Kennedy and Lynn further define

$$\begin{aligned}\Delta_\rho(q^2) &\equiv \Pi_{11}(q^2) - \Pi_{33}(q^2), \\ \Delta_1(q^2) &\equiv -[\Pi_{11}(q^2) - \Pi_{11}(0) - \Pi_{3Q}(q^2)], \\ \Delta_3(q^2) &\equiv -[\Pi_{33}(q^2) - \Pi_{33}(0) - \Pi_{3Q}(q^2)].\end{aligned}\quad (\text{C2})$$

These Δ 's determine the running of $\rho_*(q^2)$, $G_{F*}(q^2)$, and $G_{F*}(q^2)\rho_*(q^2)$ in the following way:

$$\begin{aligned}\frac{1}{\rho_*(q^2)} &= 1 - 4\sqrt{2}G_{F*}(q^2)\Delta_\rho(q^2), \\ \frac{1}{4\sqrt{2}G_{F*}(q^2)} &= \frac{1}{4\sqrt{2}G_F} - \Delta_1(q^2), \\ \frac{1}{4\sqrt{2}G_{F*}(q^2)\rho_*(q^2)} &= \frac{1}{4\sqrt{2}G_F\rho_*(0)} - \Delta_3(q^2).\end{aligned}\quad (\text{C3})$$

Note that only two of the Δ 's are independent; the three functions are related by

$$\Delta_1(q^2) - \Delta_3(q^2) = \Delta_\rho(0) - \Delta_\rho(q^2).\quad (\text{C4})$$

In our approximation (3.11), the Π 's do not contribute to the running of $e_*^2(q^2)$ and $s_*^2(q^2)$ so we only need to consider the running of $G_{F*}(q^2)$ and $\rho_*(q^2)$. The Δ 's in this approximation are given by

$$\begin{aligned}\Delta_\rho(q^2) &\approx [\Pi_{11}(0) - \Pi_{33}(0)] + q^2[\Pi'_{11}(0) - \Pi'_{33}(0)], \\ \Delta_1(q^2) &\approx -q^2[\Pi'_{11}(0) - \Pi'_{3Q}(0)], \\ \Delta_3(q^2) &\approx -q^2[\Pi'_{33}(0) - \Pi'_{3Q}(0)].\end{aligned}\quad (\text{C5})$$

Comparing with our definitions of S , T , and U in (3.12), we find

$$\begin{aligned}\alpha S &= -4e^2 \left[\frac{\Delta_3(q^2)}{q^2} \right], \\ \alpha T &= \frac{e^2}{s^2 c^2 m_Z^2} \Delta_\rho(0), \\ \alpha U &= 4e^2 \left[\frac{\Delta_\rho(q^2) - \Delta_\rho(0)}{q^2} \right] \\ &= -4e^2 \left[\frac{\Delta_1(q^2)}{q^2} - \frac{\Delta_3(q^2)}{q^2} \right],\end{aligned}\quad (\text{C6})$$

where the contribution from the reference standard model must be subtracted out from the Δ 's and the right hand sides of S and U must be evaluated at a q^2 where the approximation (C5) is valid.

In our original paper [13], we introduced a two-parameter representation of electroweak corrections using S and T . In this paper, we have presented the three-parameter generalization with the additional parameter U . Other three-parameter representations have appeared in the literature. Kennedy and Langacker [15] define their parameters h_{AZ}, h_{AW}, h_V by

$$\begin{aligned}
\alpha h_{AZ} &= -4e^2 \frac{\Delta_3(m_Z^2)}{m_Z^2}, \\
\alpha h_{AW} &= -4e^2 \frac{\Delta_1(m_W^2)}{m_W^2}, \\
\alpha h_V &= \frac{e^2}{s^2 c^2 m_Z^2} \Delta_\rho(0).
\end{aligned} \tag{C7}$$

Comparing with (C6), we find that $h_{AZ}=S$, $h_{AW}=(S+U)$, and $h_V=T$. Marciano and Rosner [14] have used the parameters $S_Z=S$, $S_W=(S+U)$, and T ; while Altarelli and Barbieri [16] have used the parameters $\epsilon_1=\alpha T$, $\epsilon_2=-\alpha U/4s^2$, and $\epsilon_3=\alpha S/4s^2$.

Almost every analysis has used a different choice of the parameters of the reference standard model. We expect that, in the future, still more choices will be used as the preferred value of the top-quark mass wanders. We hope that those who use this formalism will at least take care to state their reference point clearly.

APPENDIX D

In this appendix, we present the parameters of the fit described in Sec. VII. Numbers without errors have not been fit but chosen. We remind the reader that the dominant source of error in our evaluation of S comes not from the choice of these parameters but rather from the fact that our parametrization is too simple to provide a complete description of the e^+e^- data.

2π channel [cf. (7.14), (7.17)]:

$$\begin{aligned}
m_\rho &= 776.0 \pm 0.5 \text{ (MeV)}, \\
\frac{g_{\rho\pi\pi}^2}{48\pi} &= 0.184 \pm 0.001.
\end{aligned}$$

4π channel [cf. (7.18), (7.19)]:

$$\begin{aligned}
m &= 1710 \pm 17 \text{ (MeV)}, \\
\Gamma(m^2) &= 1440 \pm 120 \text{ (MeV)}, \\
\Gamma^{e^+e^-} &= 0.0084 \pm 0.0004 \text{ (MeV)}.
\end{aligned}$$

[$6\pi+8\pi+\dots$] channel [cf. (7.20)]:

$$\begin{aligned}
m &= 2040 \pm 7 \text{ (MeV)}, \\
\gamma &= \frac{1}{3}, \\
R_{\text{asympt}} &= 1.875.
\end{aligned}$$

3π channel [cf. (7.18), (7.24)]:

$$\begin{aligned}
m &= 1175 \pm 7 \text{ (MeV)}, \\
\Gamma(m^2) &= 387 \pm 19 \text{ (MeV)}, \\
\Gamma^{e^+e^-} &= 0.00420 \pm 0.00014 \text{ (MeV)}.
\end{aligned}$$

[$5\pi+7\pi+\dots$] channel [cf. (7.20)]:

$$\begin{aligned}
m &= 1740 \text{ (MeV)}, \\
\gamma &= \frac{1}{3}, \\
R_{\text{asympt}} &= 1.875.
\end{aligned}$$

-
- [1] M. Veltman, Act. Phys. Pol. **B8**, 475 (1977).
[2] M. Veltman, Nucl. Phys. **B123**, 89 (1977).
[3] P. Sikivie, L. Susskind, M. Voloshin, and V. Zakharov, Nucl. Phys. **B173**, 189 (1980).
[4] *Z Physics at LEP 1*, Proceedings of the Workshop, Geneva, Switzerland, 1989, edited by G. Altarelli, R. Kleiss, and C. Verzegnassi (CERN Report No. CERN-89-08, Geneva, 1989), Vol. 1.
[5] R. Renken and M. E. Peskin, Nucl. Phys. **B211**, 93 (1983).
[6] B. W. Lynn, M. E. Peskin, and R. G. Stuart, in *Physics at LEP*, LEP Jamboree, Geneva, Switzerland, 1985, edited by J. Ellis and R. Peccei (CERN Report No. CERN-86-02, Geneva, 1986).
[7] T. Appelquist, M. B. Einhorn, T. Takeuchi, and L. C. R. Wijewardhana, Phys. Lett. B **232**, 211 (1989).
[8] M. Golden and L. Randall, Nucl. Phys. **B361**, 3 (1991).
[9] B. Holdom and J. Terning, Phys. Lett. B **247**, 88 (1990).
[10] R. Johnson, B.-L. Young, and D. W. McKay, Phys. Rev. D **43**, R17 (1991).
[11] A. Dobado, D. Espriu, and M. J. Herrero, Phys. Lett. B **255**, 405 (1991).
[12] D. C. Kennedy and B. W. Lynn, Nucl. Phys. **B322**, 1 (1989); B. W. Lynn, SLAC Report No. SLAC-PUB-5077, 1989 (unpublished); M. Kuroda, G. Moulataka, and D. Schildknecht, Nucl. Phys. **B350**, 25 (1991); D. C. Kennedy, 1991 TASI Lectures (unpublished).
[13] M. E. Peskin and T. Takeuchi, Phys. Rev. Lett. **65**, 964 (1990).
[14] W. J. Marciano and J. L. Rosner, Phys. Rev. Lett. **65**, 2963 (1990).
[15] D. C. Kennedy and P. Langaker, Phys. Rev. Lett. **65**, 2967 (1990); **66**, 395(E) (1991); Phys. Rev. D **44**, 1591 (1991).
[16] G. Altarelli and R. Barbieri, Phys. Lett. B **253**, 161 (1991); G. Altarelli, R. Barbieri, and S. Jadach, Nucl. Phys. **B269**, 3 (1992).
[17] A. Ali and G. Degrossi, in *The M.A.B. Bég Memorial Volume* (World Scientific, Singapore, in press).
[18] G. Bhattacharyya, S. Banerjee, and P. Roy, Phys. Rev. D **45**, 729 (1992).
[19] An exception is the partial width $\Gamma(Z^0 \rightarrow b\bar{b})$ which receives an important vertex correction from the t quark. We will explain our treatment of this quantity in Appendix B.
[20] In Ref. [12], $Z_{Z^*}(q^2)$ and $Z_{W^*}(q^2)$ are written as $Z_{Z^*}(q^2)=[1+\kappa_{Z^*}(q^2)]^{-1}$ and $Z_{W^*}(q^2)=[1+\kappa_{W^*}(q^2)]^{-1}$.
[21] C. H. Llewellyn Smith, Nucl. Phys. **B228**, 205 (1983).
[22] Particle Data Group, J. J. Hernández *et al.*, Phys. Lett. B **239**, 1 (1990).
[23] H. Burkhardt and J. Steinberger, Annu. Rev. Nucl. Part. Sci. (to be published).
[24] A. Sirlin, Phys. Rev. D **22**, 971 (1980).

- [25] M. Consoli and W. Hollik, in *Z Physics at LEP 1* [4].
- [26] J. A. Grifols, S. Peris, and J. Sóla, *Int. J. Mod. Phys. C* **3**, 225 (1988).
- [27] M. B. Einhorn, D. R. T. Jones, and M. Veltman, *Nucl. Phys. B* **191**, 146 (1981).
- [28] S. Bertolini and A. Sirlin, *Nucl. Phys. B* **248**, 589 (1984).
- [29] T. Kinoshita, B. Nižić, and Y. Okamoto, *Phys. Rev. D* **31**, 2108 (1985); F. Jegerlehner, *Z. Phys. C* **32**, 195 (1986); B. W. Lynn, G. Penso, and C. Verzegnassi, *Phys. Rev. D* **35**, 42 (1987); H. Burkhardt, F. Jegerlehner, G. Penso, and C. Verzegnassi, *Z. Phys. C* **43**, 497 (1989).
- [30] C. Bernard, A. Duncan, J. LoSecco, and S. Weinberg, *Phys. Rev. D* **12**, 792 (1975).
- [31] S. Weinberg, *Phys. Rev. Lett.* **18**, 507 (1967).
- [32] The specific condition required is that no operator of canonical dimension 8 which appears in the operator-product expansion of the currents has a physical scaling dimension as low as 6 (for the second sum rule) or 4 (for the first).
- [33] J. Gasser and H. Leutwyler, *Ann. Phys. (N.Y.)* **158**, 142 (1984); *Nucl. Phys. B* **250**, 465 (1985).
- [34] M. Golden and L. Randall (private communication).
- [35] R. N. Cahn and M. Suzuki, *Phys. Rev. D* **44**, 3641 (1991).
- [36] R. N. Cahn and M. Suzuki, *Phys. Rev. Lett.* **67**, 169 (1991).
- [37] G. 't Hooft, *Nucl. Phys. B* **72**, 461 (1974); S. Coleman, *Aspects of Symmetry* (Cambridge University Press, Cambridge, England, 1985), Chap. 8.
- [38] V. Sidorov, in *Proceedings of the 1979 International Symposium on Lepton and Photon Interactions at High Energies*, 1979, edited by T. B. W. Kirk and H. D. I. Abarbanel (Fermilab, Batavia, 1980); L. M. Barkov *et al.*, *Nucl. Phys. B* **256**, 365 (1985).
- [39] R. Baldini-Ferrolì, in *Hadronic Physics at Intermediate Energy II*, Proceedings of the Winter School, Folgaria, Italy, 1987, edited by T. Bressani, B. Minetti, and G. Pauli (North-Holland, Amsterdam, 1987); DM2 Collaboration, D. Bisello *et al.*, in *Proceedings of the 25th International Conference on High Energy Physics*, Singapore, 1990, edited by K. K. Phua and Y. Yamaguchi (World Scientific, Singapore, 1991); in *The Hadron Mass Spectrum*, edited by E. Klempt and K. Peters (North-Holland, Amsterdam, 1991).
- [40] ARGUS Collaboration, H. Albrecht *et al.*, *Z. Phys. C* **33**, 7 (1986).
- [41] G. J. Gounaris and J. J. Sakurai, *Phys. Rev. Lett.* **21**, 244 (1968); M. Roos and J. Pišút, *Nucl. Phys. B* **10**, 563 (1969).
- [42] M. Greco, *Nucl. Phys. B* **63**, 398 (1973).
- [43] C. Bacci *et al.*, *Phys. Lett.* **86B**, 234 (1979).
- [44] M. E. Peskin, *Nucl. Phys. B* **175**, 197 (1980); J. P. Preskill, *ibid.* **B177**, 21 (1981).
- [45] E. J. Eichten, I. Hinchliffe, K. D. Lane, and C. Quigg, *Rev. Mod. Phys.* **56**, 579 (1984).
- [46] For example, M. Z. Akrawy *et al.*, *Phys. Lett. B* **242**, 299 (1990).
- [47] R. Sundrum and S. D. H. Hsu, Report No. LBL-31066, 1991 (unpublished).
- [48] T. Appelquist and O. Shapira, *Phys. Lett. B* **249**, 83 (1990).
- [49] S. F. King and S. H. Mannan, *Phys. Rev. B* **254**, 197 (1991).
- [50] M. Einhorn and D. Nash, Santa Barbara ITP Report No. NSF-ITP-91-91, 1991 (unpublished).
- [51] UA2 Collaboration, J. Alitti *et al.*, *Phys. Lett. B* **241**, 150 (1990); CDF Collaboration, F. Abe *et al.*, *Phys. Rev. Lett.* **65**, 2243 (1990); *Phys. Rev. D* **43**, 2070 (1991).
- [52] P. Langacker, in *Particle Data Group* [22], p. III. 56.
- [53] ALEPH Collaboration, D. Decamp *et al.*, *Phys. Lett. B* **265**, 430 (1991).
- [54] M. C. Noecker, B. P. Masterson, and C. E. Wieman, *Phys. Rev. Lett.* **61**, 310 (1988); S. A. Blundell, W. R. Johnson, and J. Sapirstein, *ibid.* **65**, 1411 (1990).
- [55] P. G. H. Sandars, *J. Phys. B* **23**, L655 (1990).
- [56] L. M. Krauss, *Phys. Lett. B* **269**, 407 (1991).
- [57] V. A. Dzuba, V. V. Flambaum, and O. P. Sushkov, *Z. Phys. D* **1**, 243 (1986); C. Monroe, W. Swann, H. Robinson, and C. E. Weiman, *Phys. Rev. Lett.* **65**, 1571 (1990).
- [58] We make the simplistic assumption that the probability distribution corresponds to each measurement is Gaussian. We also ignore the correlations between the various measurements; we believe that this is a good assumption for the subset of observables we have chosen.
- [59] D. Decamp *et al.*, *Z. Phys. C* **53**, 1 (1992).
- [60] This remark follows the spirit of D. Levinthal, F. Bird, R. G. Stuart, and B. W. Lynn, Report No. CERN-Th-6094-91 (unpublished).
- [61] S. Bertolini and A. Sirlin, *Phys. Lett. B* **257**, 179 (1991).
- [62] E. Gates and J. Terning, *Phys. Rev. Lett.* **67**, 1840 (1991).
- [63] M. J. Dugan and L. Randall, *Phys. Lett. B* **264**, 154 (1991).
- [64] H. Georgi, *Nucl. Phys. B* **363**, 301 (1991).
- [65] A. Blondel *et al.*, *Z. Phys. C* **45**, 361 (1990).